CHAPTER IV

RESULTS AND DISCUSSION

4.1 Introduction

This study present comprehensive studies about the effect of polymer concentration, effect of type of surfactants which are CTAB (cationic), Triton X-100 (non-ionic) and SDS (anionic) with different concentration (1 wt.% to 3 wt.%) towards the membrane performances, morphology, thermal analysis and physico-chemical properties. The RO performances of studied membranes in terms of pure water permeation (PWP), saline water flux and salt rejection were investigated. The experiments of saline water were conducted using six concentration which were 2 000, 5 000, 10 000, 30 000, 40 000, and 50 000 ppm. SEM was used to study the morphology of membranes. Thermal analysis and physico-chemical properties of the membranes had been analyzed using TGA and FTIR, respectively.

4.2 Effect of Polymer Concentration on Reverse Osmosis Membrane Performance

Membrane formulation greatly influenced the performance of RO membrane. Composition of the polymer in membrane solution will affect the performance of the resultant membrane. Thus, the first factor that had been studied in this study is polymer concentration. The effect of polysulfone (PSF) concentration on RO membrane performances were evaluated in terms of pure water permeation (PWP) and desalination performance.

Figure 11 shows the effect of PSF concentration on saline water flux of RO membrane. The PWP of membranes were investigated using distilled water, represented by 0 ppm of saline water. From the result obtained, membrane PSP1 produced highest PWP which was 6.38 L/m^{2}h. According to Anne (2008), the high permeability characteristics generally indicates a high porosity of the membrane. Meanwhile, by increasing the polymer concentration which is membrane PSP3 reduced the PWP to 4.11 L/m^{2}h. The reduction of the PWP was about 35.6 % when the two membranes were compared. Increasing the polymer concentration in the dope solution increased the thickness of the membrane and reduced its porosity, consequently resulting in the declination of permeability rate. Thus, a higher polymer concentration membrane would promote a lower water permeability (Sofiah et al., 2010).

For saline water flux, membrane PSP1 achieved higher flux as compared to membrane PSP3 for all saline water concentration. This was due to an increase of polymer concentration caused the skin layer of asymmetric membrane to be denser and thicker.

Hence, the volume of flux produced was reduced (Ismail & Hassan, 2006). By comparing the concentration of saline water, 2 000 ppm produced highest flux which was 26.79 L/m^{2}h and the lowest flux achieved by 40 000 ppm which was 1.25 L/m^{2}h. This phenomenon might due to the amount and size of molecule in salt solution. As saline water concentration increased, the amount and size of molecule increased. Hence it reduced the flux produced by the membranes.

FIGURE 11: Effect of PSF concentration on saline water flux of RO membrane

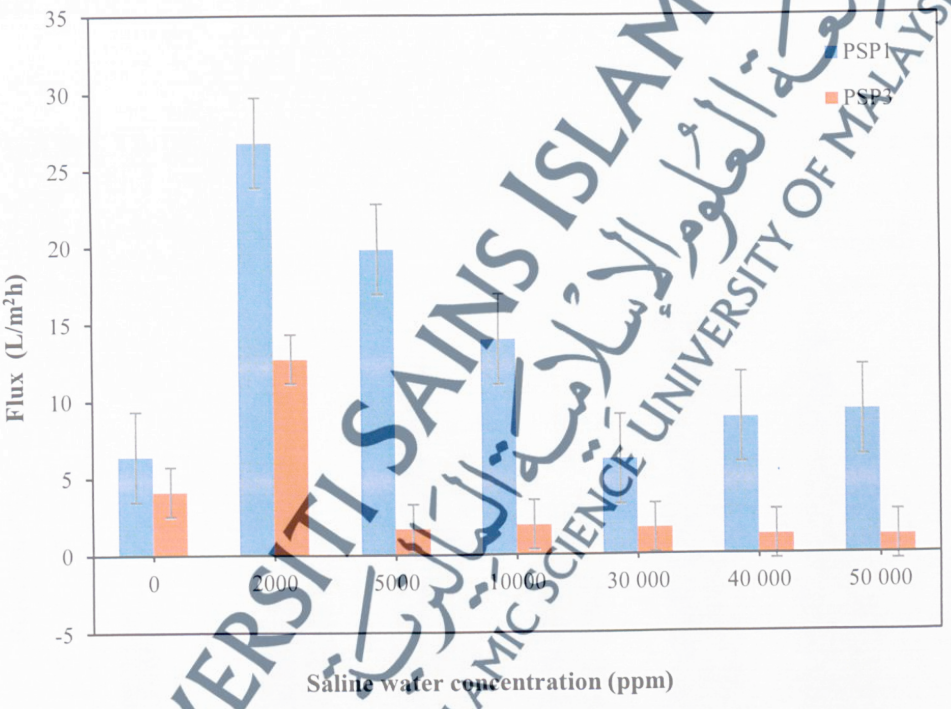

Meanwhile, for saline water rejection, the effect of PSF concentration on RO membrane was demonstrated in Figure 12. It was clearly seen that salt rejection decline as the polymer concentration increased. Membrane PSP1 produced highest salt rejection of about 87.25 % at 40 000 ppm concentration of saline water. The lowest salt rejection produced by membrane PSP3 at 2 000 ppm concentration of saline water which was

74.05 %. This trend was in agreement with the result reported by previous study for the case of polyethersulfone membrane (Sofiah et al., 2010). An increase in the polymer concentration results in significant increase in solution viscosity of PSF dope solution. This phenomenon will lead to a higher mass transfer resistance between the non-solvent (precipitation bath) and the solvent (NMP) in the system during solidification of the casting solution. Thus, at high polymer concentration, the precipitation process stops after a longer period of time, which leads to the formation of denser and compact structure, subsequently leads to a lower porosity and selectivity of membrane (Ahmad et al., 2014).

FIGURE 12: Effect of PSF concentration on saline water rejection of RO membrane

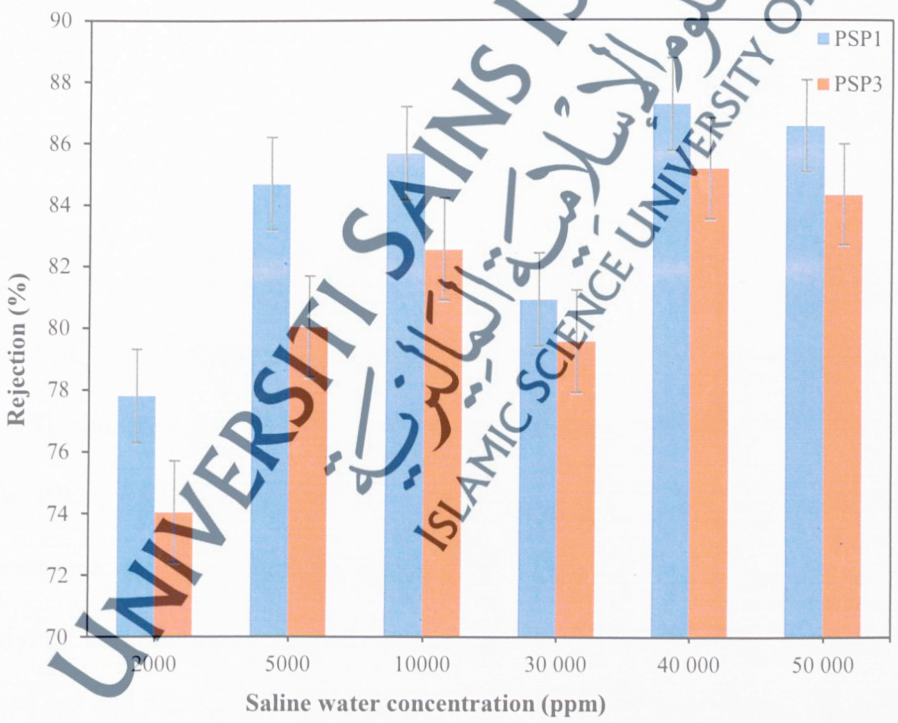

4.3 Effect of Polymer Concentration with Surfactant on Reverse Osmosis Membrane Performance

Addition of surfactant in the casting solution can influence the structure and performance of the membranes. For hydrophilic coagulant, hydrophilic surfactant can improve the formation of macrovoids and the hydrophilicity of membranes. However lipophilic does not possess these properties. On the other hand, for a lipophilic coagulant, lipophilic surfactant are more effective in changing membrane structure than hydrophilic surfactants. Thus the formation of macrovoids can be controlled (Tsai et al, 2000). In addition, positively or negatively-charged surfactants may slightly change the membrane surface charge due to their charges, and results in altering performance of the membrane (Rahimpour, 2007). 2.0 wt. % of CTAB, Triton X-100 and SDS had been chosen as optimum concentration of surfactant to be added into the casting solution of membrane PSP1 and PSP3.

The polymer concentration and the type of surfactant had important influence on the PWP (0 ppm of saline water) and saline water flux. Figure 13 demonstrated the effect of PSF concentration with 2 wt. % of surfactant on saline water flux of RO membrane. For PWP, PSP1-S2 achieved the highest volume of PWP as compared to other membrane which was 24.98 L/m^2h. Meanwhile for saline water flux, in terms of polymer concentration, membranes that contained 21 % of PSF which were PSP1-C2, PSP1-T2 and PSP1-S2 produced higher flux compared to membrane that contained 23 % of PSF. This result was might be due to the fact that an increase in the initial polymer concentration in the casting solution leads to a much higher polymer concentration at the surface. This implies that the volume fraction of polymer increases and,

consequently, a lower porosity is obtained (Tsai, 2000). Moreover, addition of small amount of surfactants in the casting solution increases the porosity of the membrane support layer, hence enhance the permeate flux (Rahimpour, 2007). In the context of surfactant type, membrane with CTAB, which is PSP1-C2 produced highest flux which is 29.19 L/m^{2}h in 40 000 ppm of saline water as compared to other surfactant.

FIGURE 13: Effect of PSF concentration with 2.0 wt. % surfactant on saline water flux of RO membrane

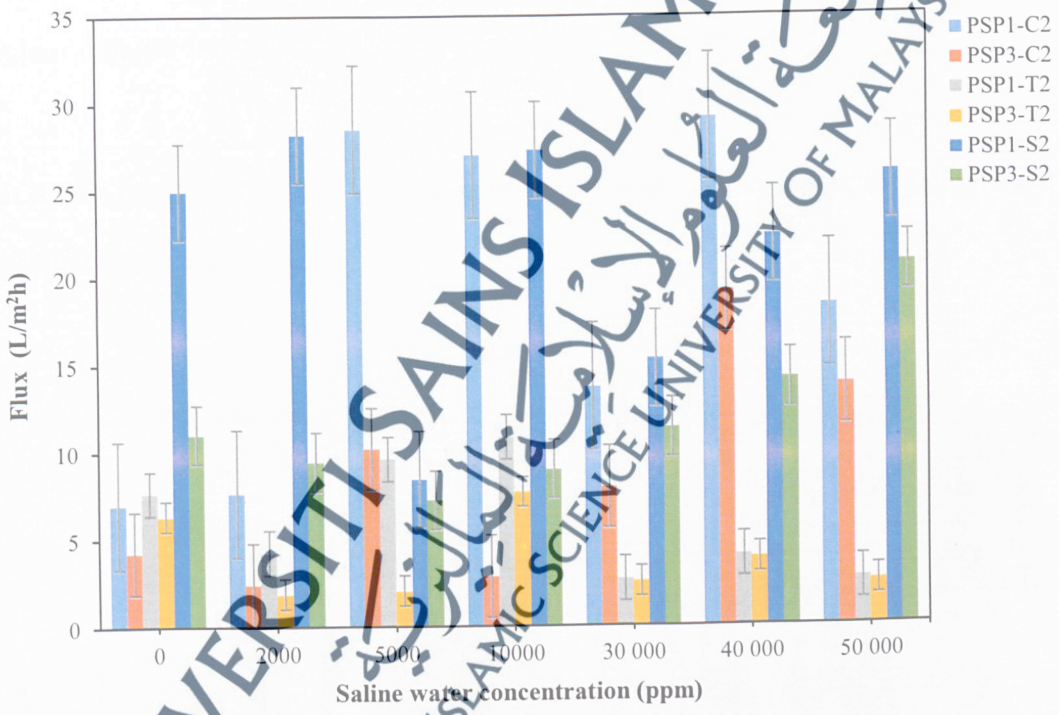

Figure 14 shows the effect of PSF concentration with 2.0 wt. % surfactant on saline water rejection of RO membrane. It had been shown that lower concentration of polymer used in the membrane produced higher salt rejection as compared to higher polymer concentration. The highest salt rejection achieved by membrane PSP1-C2 of about 94.08 %. This result was acceptable as it was in the range of salt rejection that

produced by commercial RO membrane. For example, membrane series AG from GE Osmonics produced 95.5 % salt rejection in brackish water using polyamide polymer. Meanwhile, membrane PSP3-C2 produced the lowest salt rejection which was 76.5 %. This was due to the effect of polymer concentration in the membrane solution. However, the salt rejection was still higher than membrane PSP3 which do not contain surfactant which was 74.05 %. It shown that addition of small amount of surfactant improved the salt performance of the membranes. In terms of surfactant type, membrane with CTAB, which is membrane PSP1-C2 achieved highest salt rejection. By comparing from both experiments, membrane PSP1-C2 appeared to be the best membrane as it produced highest flux (29.19 L/m^{2}h) and highest salt rejection (94.08%).

FIGURE 14: Effect of PSF concentration with 2.0 wt. % surfactant on saline water rejection of RO membrane

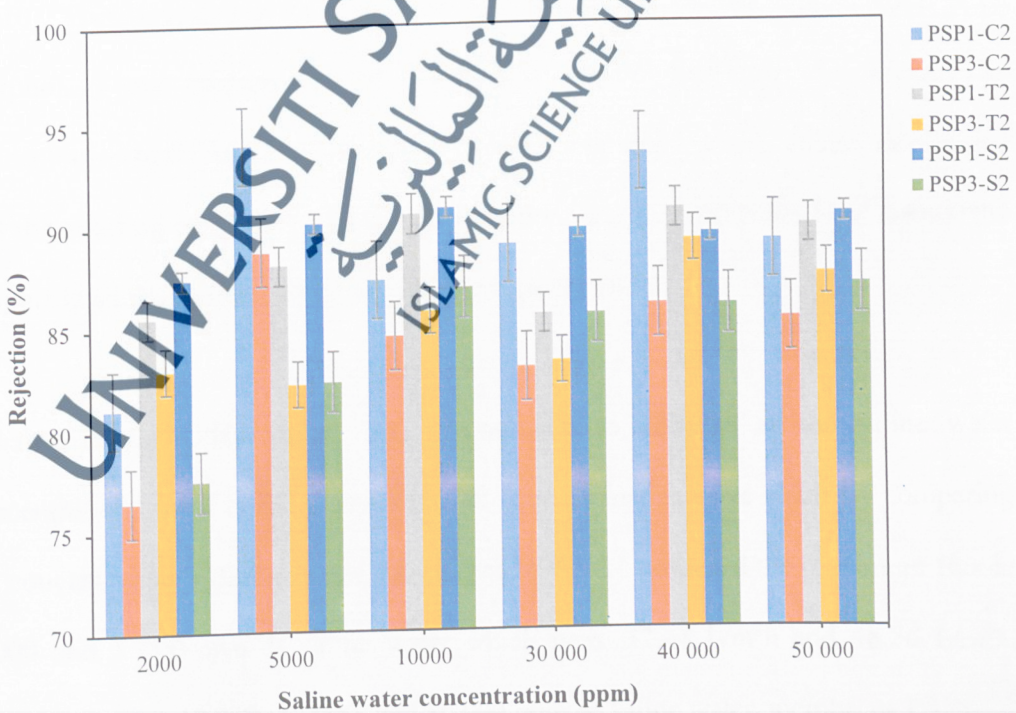

4.4 Effect of CTAB as Cationic Surfactant on Reverse Osmosis Membrane Performance

Cetyl trimethylammonium bromide (CTAB) was selected as strong cationic surfactant to be studied on the RO performance of PSF membrane. Figure 15 exhibit the effect of CTAB concentration on saline water flux of RO membrane. The PWP of the membranes were represented by 0 ppm concentration of saline water. Presence of CTAB in the casting solution increases the PWP. Membrane PSP1-C1 achieved the maximum value of PWP which was 34.64 L/m^{2}h. Increasing CTAB concentration more than 1 wt. % resulted in decreasing the PWP. This might due to the high viscosity of casting solution that prevents the penetration of non-solvent and weaken the macrovoids formation, hence lead to low permeability of membrane (Teoh and Chung, 2009). On the other hand, after the addition of 2 wt. % of CTAB which was membrane PSP1-C2, the PWP increases gradually. This finding correspond with result of Mulijani et al. (2010). They investigate the effect of CTAB as additive in the casting solution on morphology and performance of asymmetric CA-PS composite membrane. The concentration of CTAB that had been used were 0.5 up to 2.0 wt. %. The result reported that the addition of CTAB in the casting solution increases the porosity of membrane support layer and results in higher pure water permeation.

Meanwhile, for saline water flux, the trend were different as the saline water concentration varied in the experiments. It showed inconclusive result by comparing the concentration of saline water. Membrane PSP1-C1 produced the maximum flux in 2 000 and 5 000 ppm of saline water which were 32.48 L/m^{2}h and 48.56 L/m^{2}h, respectively. For 10 000, 30 000, and 50 000 ppm of saline water, membrane PSP1-C3

achieved the highest volume of flux which were 54.13 L/m^{2}h, 55.28 L/m^{2}h and 27.35 L/m^{2}h, respectively. On the other hand, membrane PSP1-C2.5 produced highest flux at 40 000 ppm of saline water which was 48.11 L/m^{2}h. The best membrane in terms of saline water flux was membrane PSP1-C3 which produced 55.28 L/m^{2}h in 30 000 ppm of saline water. According to Rahimpour et al. (2007), by increasing the concentration of CTAB, the porosity of membrane support layer increased, hence lead to higher permeate flux produced.

FIGURE 15: Effect of CTAB concentration on saline water flux of RO membrane

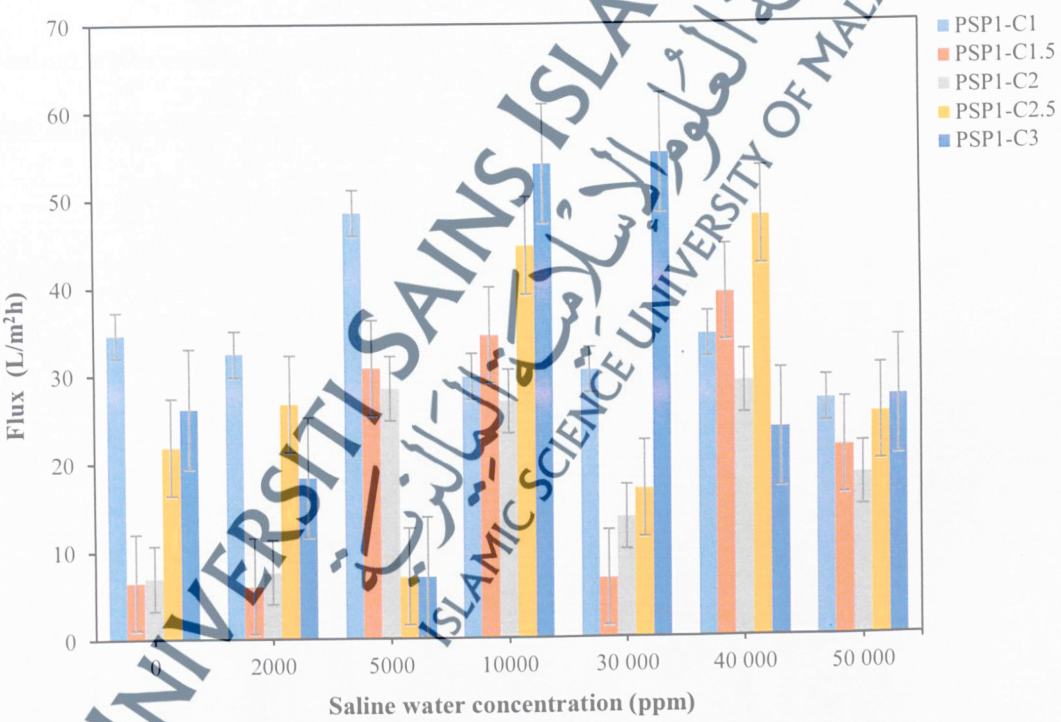

Figure 16 demonstrated the effect of CTAB concentration on saline water rejection of RO membrane. The salt rejection obtained from these membranes were in the range of 75 % to 94 %. The highest salt rejection produced by membrane PSP1-C2 for all the concentration of saline water which were 81.1% (2 000 ppm), 94.08 % (5 000 ppm),

87.4 % (10 000 ppm), 89.05 (30 000 ppm), 93.48 % (40 000 ppm) and 89.1 % (50 000 ppm). Overall, it is clearly seen that the salt rejection decreased in the addition of 1.5 wt. % CTAB which is membrane PSP1-C1.5. This was might due to at 1.5 wt. % of CTAB, the surfactant molecules prefer to form micelles in comparison with polymer-surfactant complex, therefore higher casting solution viscosity result in lower membrane porosity and higher skin layer thickness. Increasing CTAB concentration to 2 wt. % which is membrane PSP1-C2, resulted in salt rejection increased, reaches its maximum value for all saline water concentration because the membrane porosity had increased and lower the skin layer thickness (Saedi et al, 2012). It was indicated that 2 wt. % is the optimum concentration of CTAB in producing high salt rejection. In terms of saline water concentration, 5 000 ppm obtained highest salt rejection as compared to other concentrations which was 94.08 %.

FIGURE 16: Effect of CTAB concentration on saline water rejection of RO membrane

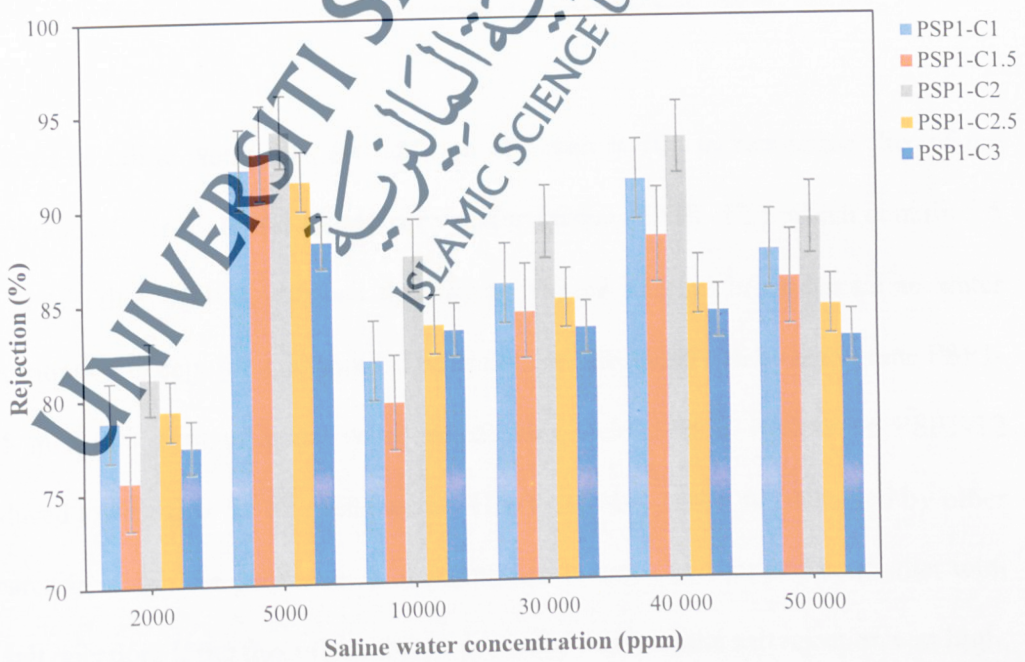

4.5 Effect of Triton X-100 as Non-Ionic Surfactant on Reverse Osmosis Membrane Performance

Triton X-100 was used as nonionic surfactant in the membrane formulation. The effect of Triton X-100 concentration on saline water flux of RO membrane is shown in Figure 17. The PWP represented by 0 ppm of saline water concentration. By introducing 1 wt. % of Triton X-100 which was membrane PSP1-T1, the PWP reaches the maximum volume which is 32.48 L/m^{2}h. Increasing Triton X-100 concentration more than 1 wt. % resulted in declination of PWP. Membrane PSP1-T1.5 produced the lowest PWP which gave value of 6.06 L/m^{2}h. This was contrast with the result obtained from previous study by Rahimpour et al (2007). It had been reported that increasing of Triton X-100 concentration increases the PWP for polyethersulfone (16 wt. %) ultrafiltration membrane. This was might due to the different concentration and type of polymer used in previous and this study. As mentioned in the PSF concentration experiments, increasing of polymer concentration resulted in declination of PWP.

In terms of saline water flux, the addition of Triton X-100 increased the flux of the membranes. Overall, it was clearly seen that membrane PSP1-T2.5 which contain 2.5 wt. % of Triton X-100, obtained the highest volume of flux in all the saline water concentration except for 2 000 ppm. The maximum flux produced by membrane PSP1-T2.5 in 5 000 ppm of saline water which was 26.51 L/m^{2}h. Membrane PSP1-T2 produced lowest flux for all saline water. This trend was commonly obtained by other research in which the performance of membrane in terms of flux was contradict with the salt rejection. If the flux of membrane produced was low, the salt rejection was high.

In this case, it can be proven that membrane PSP1-T2 produced lowest flux, but achieved highest salt rejection (Figure).

FIGURE 17: Effect of Triton X-100 concentration on saline water flux of RO membrane

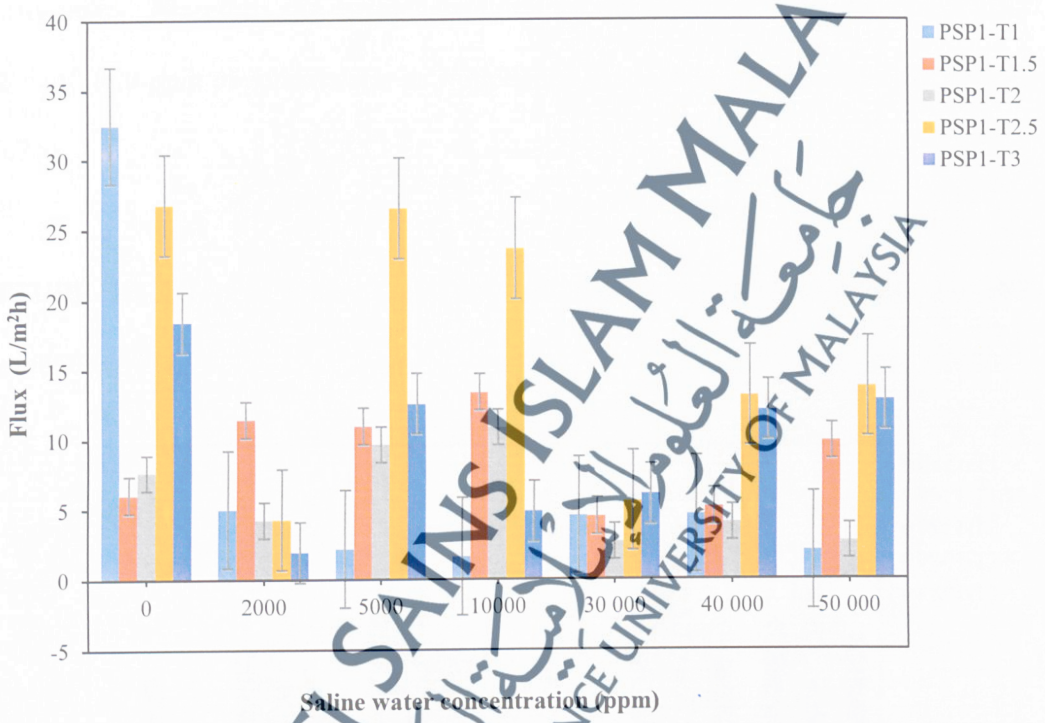

The effect of Triton X-100 concentration on saline water rejection was illustrated in Figure 18. The trend of the salt rejection were similar for all saline water concentration, in which the salt rejection increased as the Triton X-100 concentration increased, and achieved the highest rejection at 2 wt. % of Triton X-100 concentration, which represented by membrane PSP1-T2 which were 85.6 % (2000 ppm), 88.16 % (5 000 ppm), 90.6 % (10 000 ppm), 85.57 % (30 000 ppm), 90.7 % (40 000 ppm) and 89.86 % (50 000 ppm). On the other hand, by increasing Triton X-100 concentration more

than 2.5 wt. %, the salt rejection decreased. It was reported by Rahimpour et al. (2007) that when the surfactant concentration increased, the non-polar tail of surfactant molecules settle beside one another and form micelles with polar groups in outer surface and non-polar groups inside the micelles in addition to the polymer surfactant complex. These free micelles deteriorate the membrane structure and decrease the membrane performance. Therefore, the optimal condition for salt rejection was membrane PSP1-T2 in 40 000 ppm of saline water as it produced the highest salt rejection which was 90.7 %.

FIGURE 18: Effect of Triton X-100 concentration on saline water rejection of RO membrane

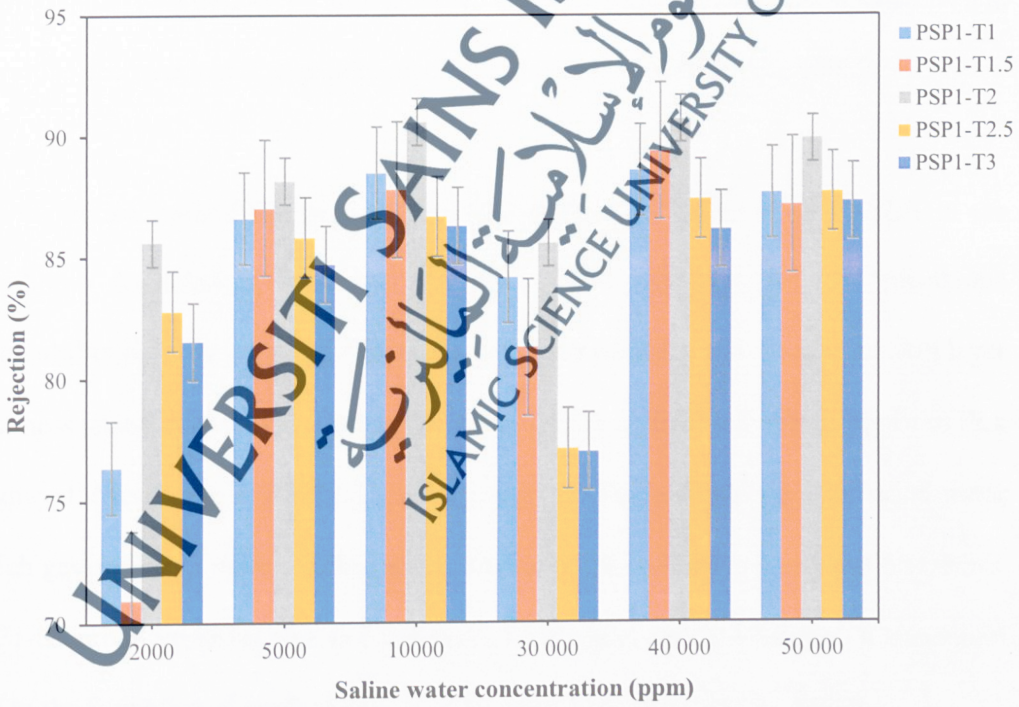

FIGURE 19: Effect of SDS concentration on saline water flux of RO membrane

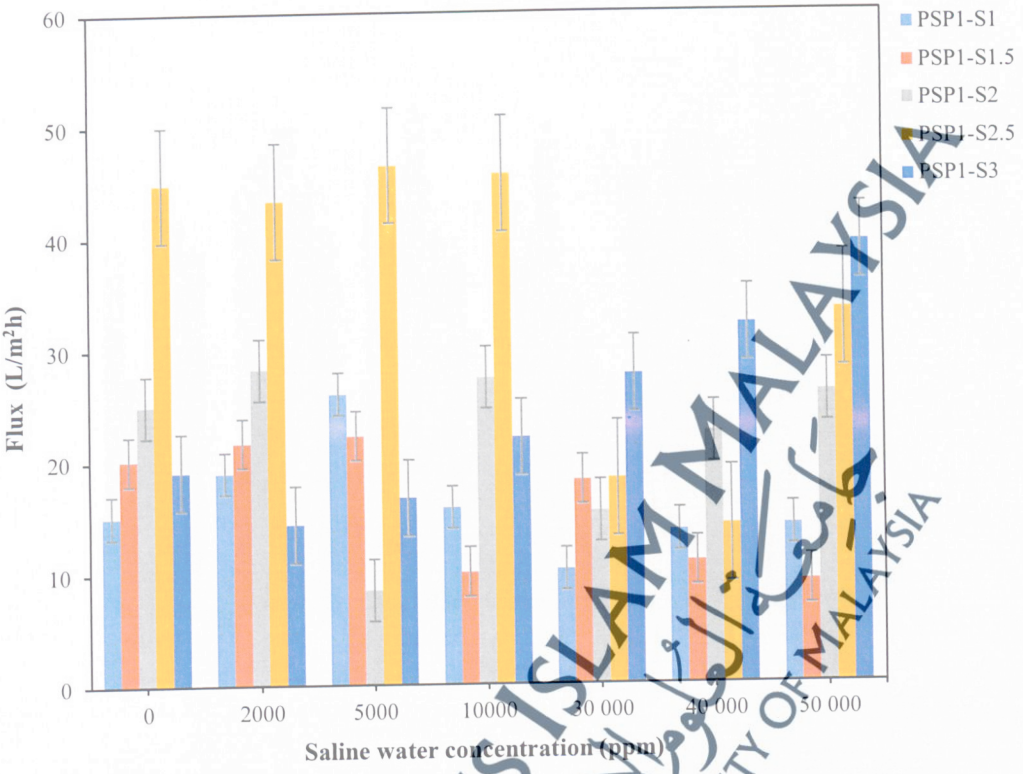

Figure 20 exhibits the effect of SDS concentration on saline water rejection of RO membrane. The salt rejection increased after the addition of SDS in the membrane formulation for all saline water concentration. The optimum concentration of SDS is 2 wt. %, which was membrane PSP1-S2, which achieved the highest value of salt rejection for all saline water concentration. Membrane PSP1-S2 obtained maximum salt rejection of about 90.9 % in 10 000 ppm of saline water. Then, by increasing the SDS concentration more than 2.5 wt. %, the salt rejection declined. This result was similar with those obtained in Figure and Figure. High concentration of surfactant used lead to declination of salt rejection.

FIGURE 20: Effect of SDS concentration on saline water rejection of RO membrane

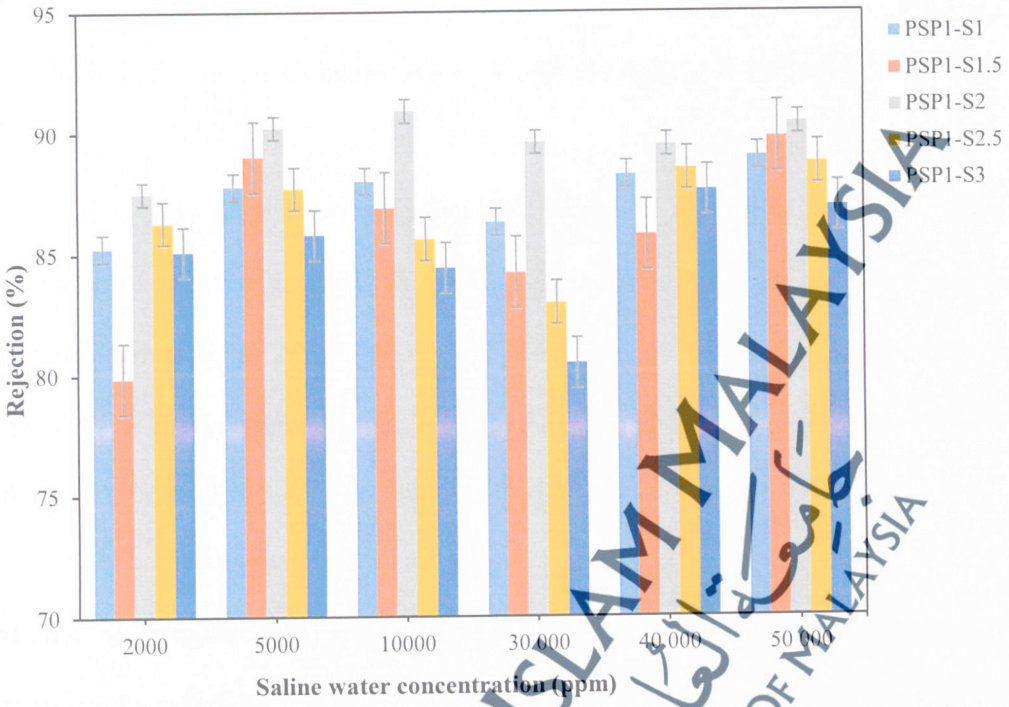

4.7 Morphological Study using Scanning Electron Microscope (SEM)

4.7.1 Effect of Polymer Concentration on Morphology of Membrane

In this study, all the fabricated membranes exhibit asymmetric structures with a combination of two layers, which are active layer and supporting layers. Both layers play significant role in membrane performance. Sofiah et al (2010) stated that composition of the polymer in membrane solution will affect the performance of the resultant membrane as it plays a role in improving macrovoid structure and thickness.

SEM cross-sectional images of membrane PSP1 was shown in Figure 21. Membrane PSP1 showed a skin layer that was well-developed and supported by a porous support layer with large finger-like and macrovoid structure. According to Sofiah et al (2010) that had studied the polymer concentration in UF membrane, lower polymer concentration used in the dope preparation lead to an increasing of macrovoids formation. This was due to the solvent-non solvent exchange, leading to the different starting conditions for phase separation at layers far from the surface. The formation of macrovoids is favoured when non-solvent diffusion rate into the polymer-poor phase being formed exceeds the rate of outward-solvent diffusion rate. The growth of a thin polymer layer resulted from the lower polymer concentration and strong interaction between PSF and water. Water is claimed to be a strong non-solvent for PSF polymer and the coagulation process will occur faster when the polymer solution is brought into contact with water and the finger-like structure formed. Generally, the large finger-like macrovoids are formed when the coagulation process is faster (Sofiah et al, 2010).

Figure 22 demonstrated the SEM cross-sectional images of membrane PSP3. Compared to membrane PSP1, it displayed denser skin layer and smaller finger-like structure and macrovoids. Used of a more concentrated polymer enhanced the viscosity of the dope solution, leading to the formation of smaller pore size. This phenomenon occured since high viscosity would prevent the diffusion exchange rate of solvent and non-solvent in sub-layer inducing fast-phase separation at the skin layer and slows the precipitation rate of the sub-layer. Therefore, this results in the formation of an asymmetric membrane with dense and thick skin layer supported by a closed cell sub-layer. Besides, higher polymer concentration induced the chain entanglement and therefore reduced the formation of the macrovoids in the skin layer (Sofiah et al., 2010).

(i) Membrane PSP1

FIGURE 21: SEM cross-sectional images of membrane PSP1

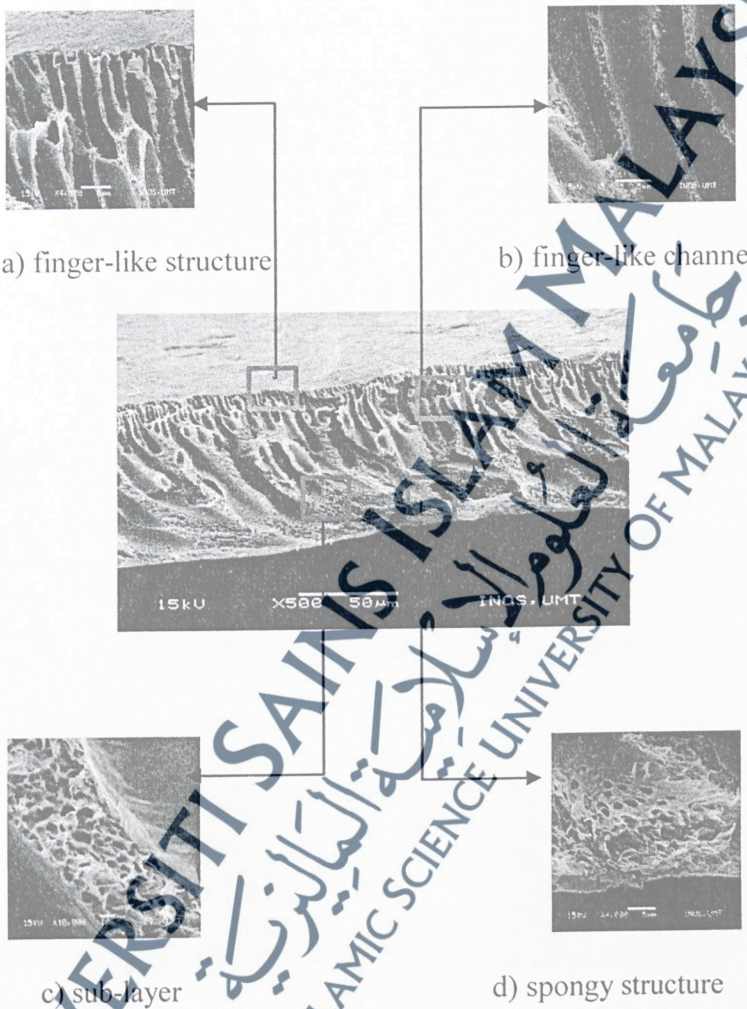

(ii) Membrane PSP3

FIGURE 22: SEM cross-sectional images of membrane PSP3

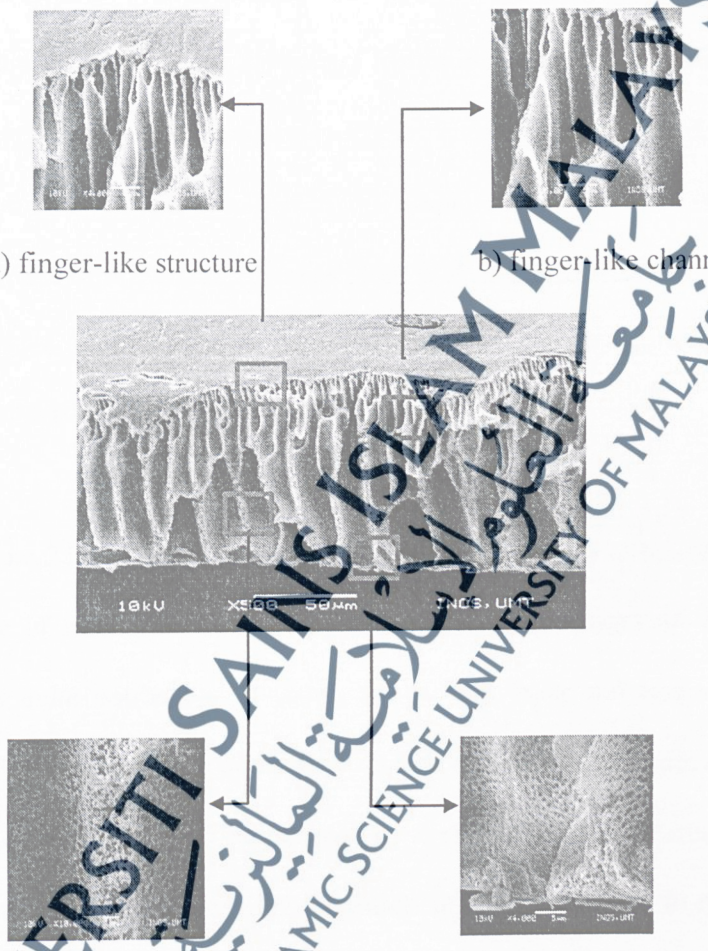

4.7.2 Effect of Polymer Concentration with Surfactant on Morphology of Membrane

As shown in Figure 23, the cross-sectional morphology of membrane PSP1-C2 was observed by SEM at 500 x, 4000 x, 5000 x, and 10 000 x magnification for the overall cross-section, finger-like and spongy structure, finger-like channel and sub layer, respectively. The membrane exhibits a dense toplayer (skin layer and microvoids) and a porous sub layer (finger-like pore and macrovoids). Microvoids seemed to be closed pore structure and did not interconnected with other pores. The large size of macrovoids enhance the permeability performance of the membrane, which gave the highest value of PWP and flux.

Meanwhile, Figure 24 presented the SEM cross-sectional images of membrane PSP3-C2. The change of membrane morphological structure by increasing the polymer concentration is quite noticeable. It shows denser top layer and larger finger-like structure. In addition, the number of macrovoids was also found to disappear gradually. As mentioned earlier, using of higher polymer concentration induced the chain entanglement and therefore reduced the formation of the macrovoids in the sublayer. This leads to the lower performance of the membrane.

(i) Membrane PSP1-C2

Figure 23: SEM cross-sectional images of membrane PSP1-C2

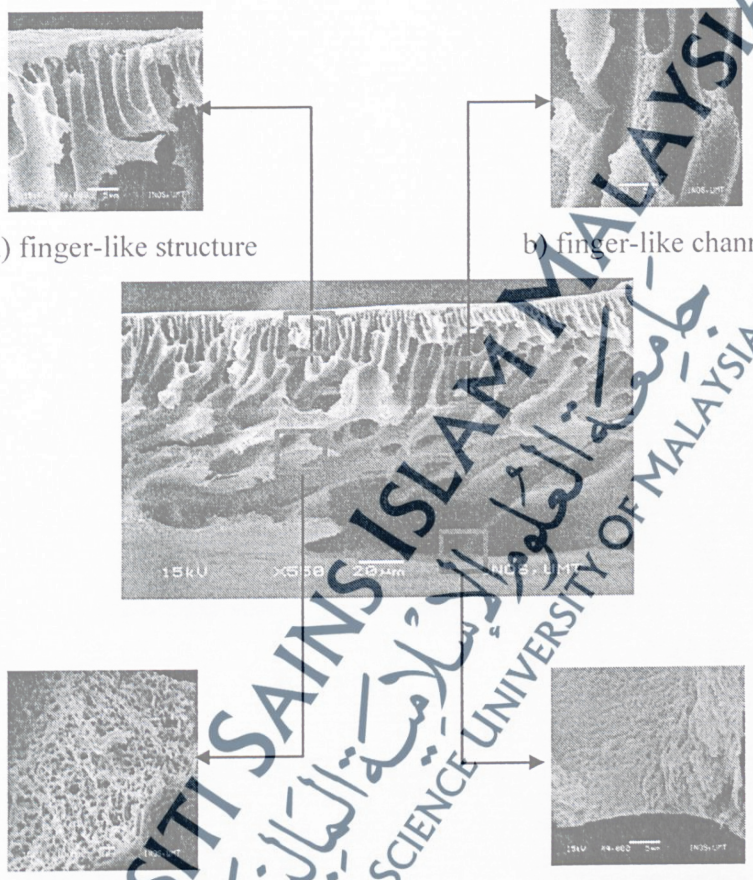

(ii) Membrane PSP3-C2

FIGURE 24: SEM cross-sectional images of membrane PSP3-C2

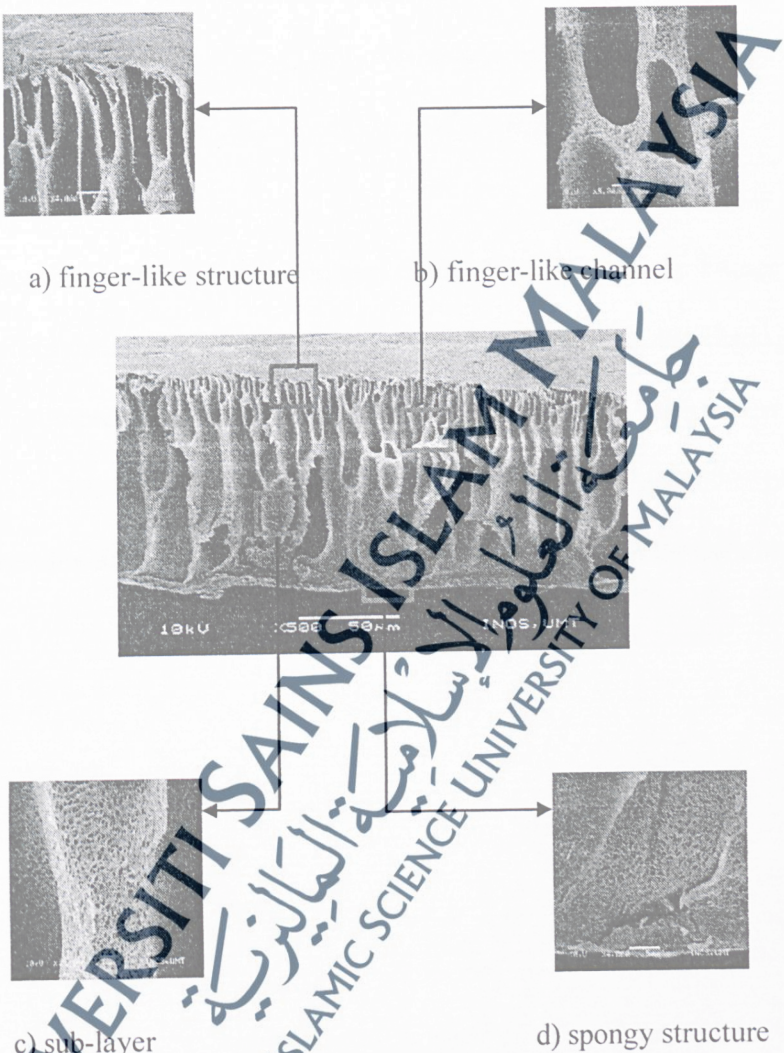

Figure 25 demonstrated the SEM cross-sectional images membrane PSP1-T2. The membrane exhibited thinner skin layer and more porous spongy sub layer as compared to membrane PSP1. The presence of triton X-100 as additive in the casting solution caused the formation of fully developed finger-like pores in the sub layer which were larger than pores exists in the membrane PSP1. This structure improved the performance in terms of PWP, flux and salt rejection of the membrane.

SEM cross-sectional images of membrane PSP3-T2 is shown in Figure 26. The increasing of polymer concentration which was 23 % of PSF in the casting solution resulted in a compressed structure with thicker skin-layer in comparison with the membrane PSP1-T2. The pores produced did not interconnected with other pores. This phenomena resulted in decreasing of water and salt permeation of the membrane.

(iii) Membrane PSP1-T2

Figure 25: SEM cross-sectional images of membrane PSP1-T2

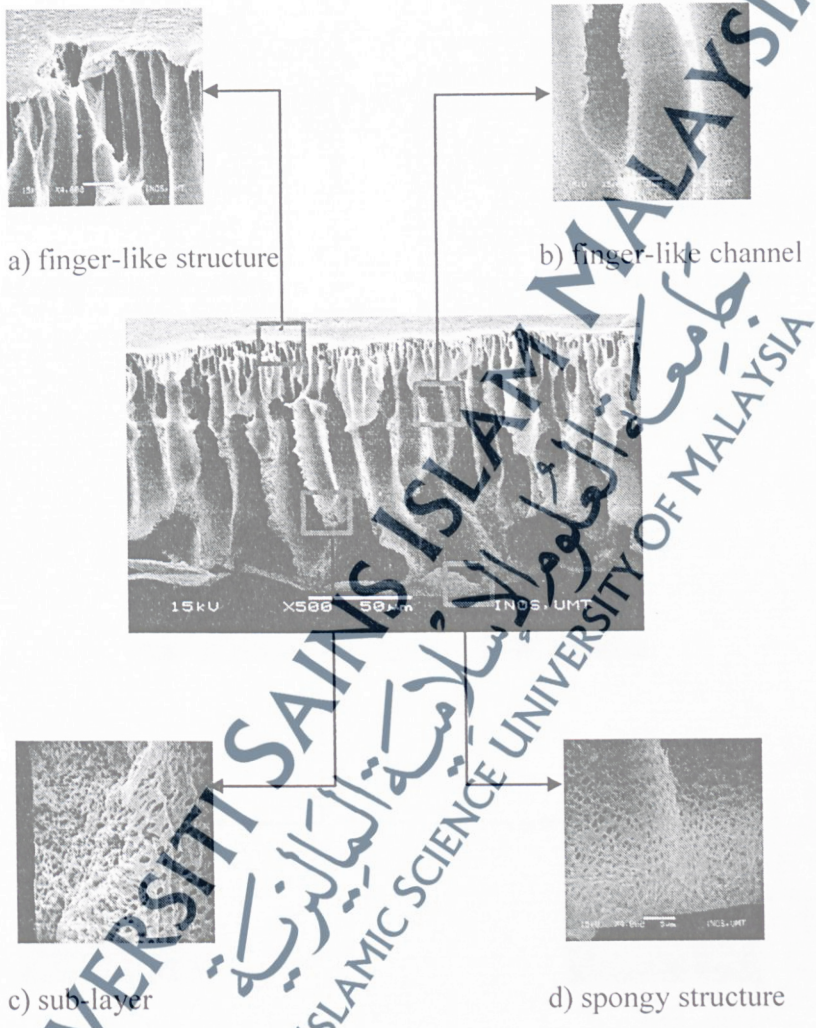

(iv) Membrane PSP3-T2

FIGURE 26: SEM cross-sectional images of membrane PSP3-T2

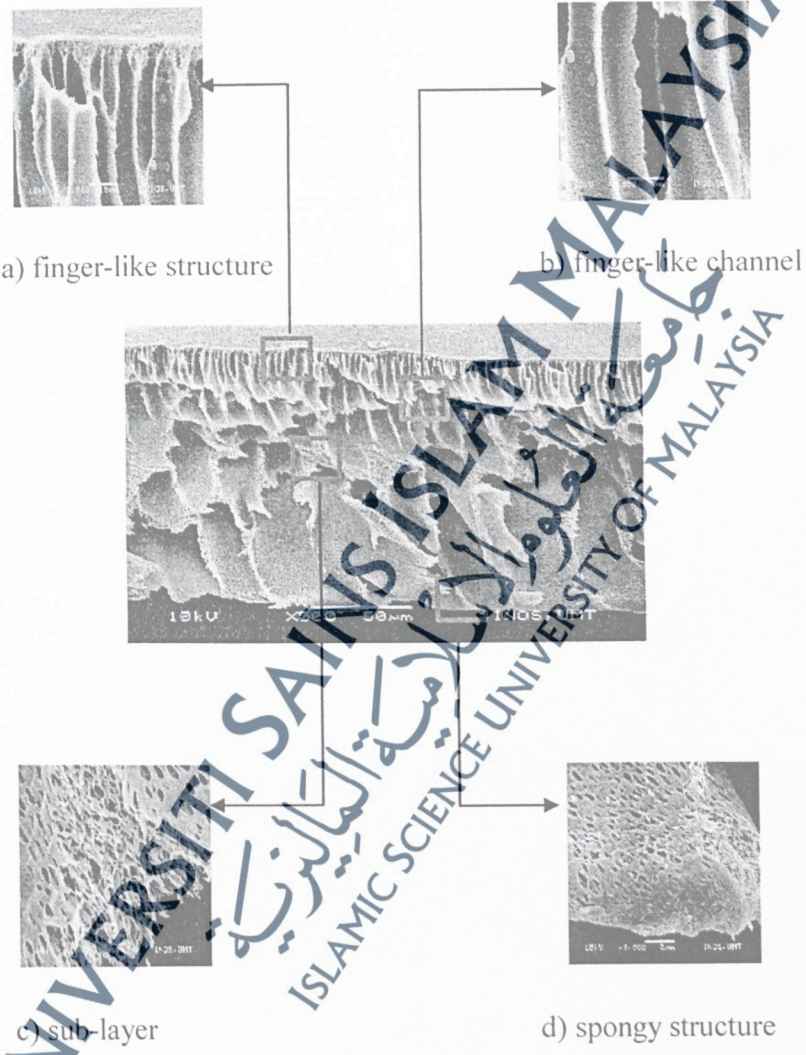

SEM cross-sectional images of membrane PSP1-S2 and membrane PSP3-S2 were depicted in Figure 27 and Figure 28, respectively. It was apparent that both membrane exhibit a characteristic morphology of asymmetric membrane which consist of a dense top layer and porous sub-layer.

In particular, membrane PSP1-S2 produced large macrovoids, hence improve the permeability performance of the membrane. Meanwhile, for membrane PSP3-S2, it exhibited denser top layer and fully develop finger-like structure in sub layer of membrane. Number of pores produced increased as compared to membrane PSP1-S2. The spongy structure gradually become compact. It reduced the porosity of membrane support layer and resulted in lower PWP and salt performance.

(v) Membrane PSP1-S2

FIGURE 27: SEM cross-sectional images of membrane PSP1-S2

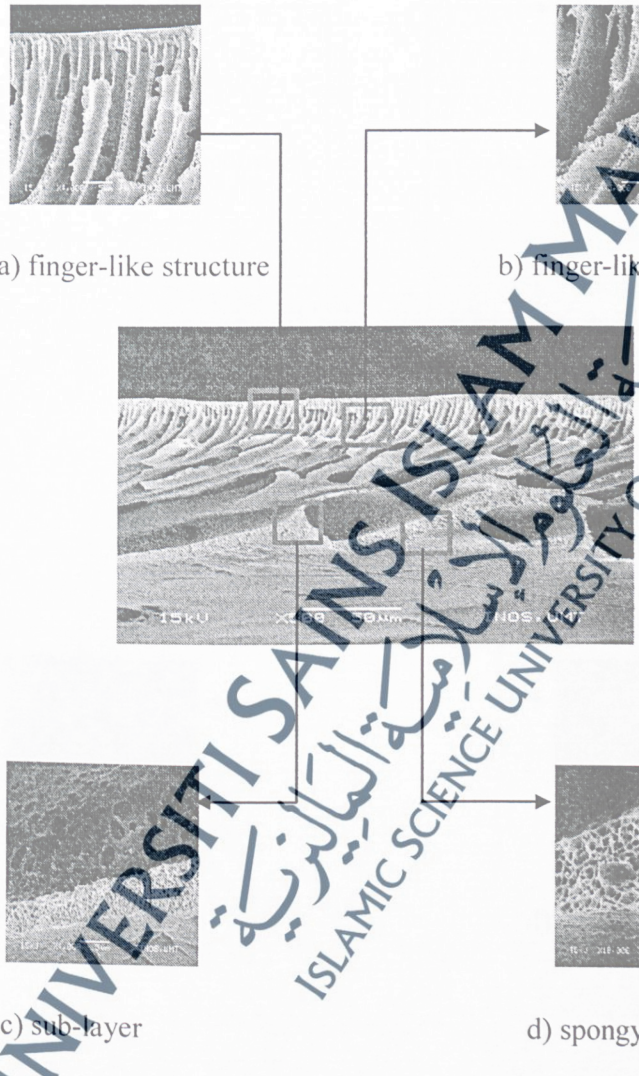

a) finger-like structure

b) finger-like channel

c) sub-layer

d) spongy structure

(vi) Membrane PSP3-S2

FIGURE 28: SEM cross-sectional images of membrane PSP3-S2

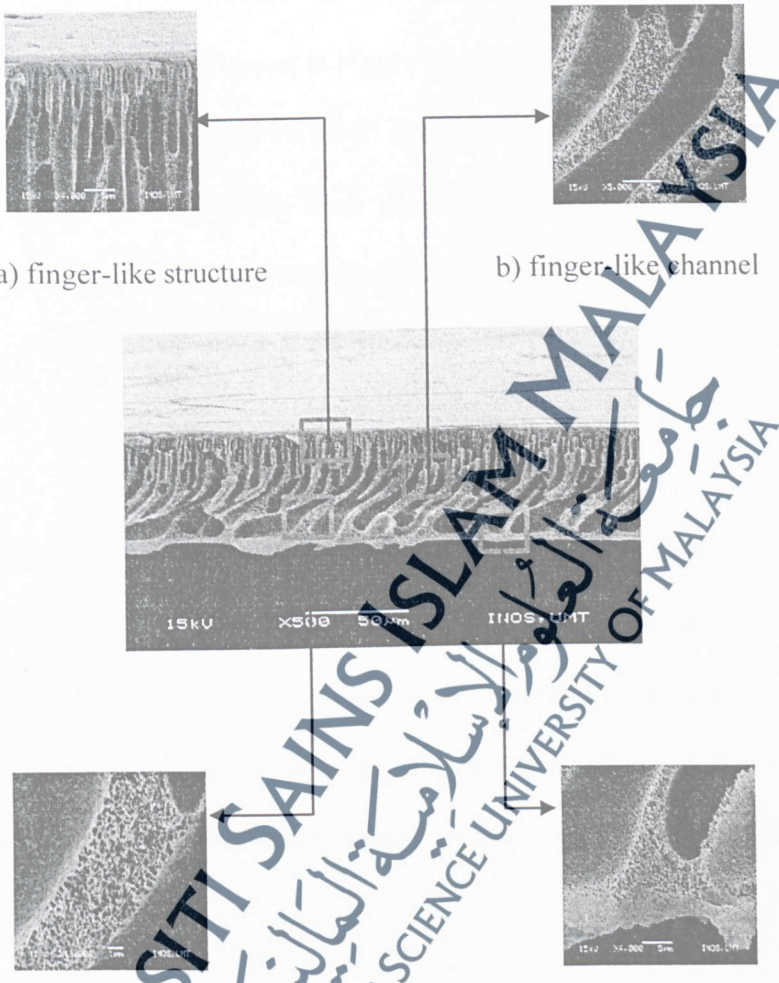

4.7.3 Effect of CTAB Concentration on Morphology of Membrane

SEM cross-section images of the prepared membranes with different concentrations of CTAB were shown in Figure 29 until Figure 32. Addition of 1 wt. % of CTAB which was membrane PSP1-C1 (Figure 29) resulted in membrane with significantly thinner skin-layer and more porous sub layer compared to membrane PSP1. Formation of polymer-surfactant complex decreased the degree of polymer chain entanglement, therefore the penetration of non-solvent into the chain spaces can be increased and formation of macrovoids enhances (Saedi et al., 2012).

Meanwhile, as the concentration of CTAB increases up to 1.5 wt. % (membrane PSP1-C1.5) in the casting solution, the top layer become thicker and the macrovoids suppressed (Figure 30). This was because higher surfactant concentration resulted in higher casting solution viscosity that prevents the penetration of nonsolvent, and weakens macrovoids formation and therefore decreases membrane porosity (Saedi et al., 2012).

When the CTAB concentration reached 2 wt. %, large macrovoids appeared and membrane porosity increased again (Figure 23). It had been discussed that the microvoids seemed to be closed pore structure and did not interconnected with other pores. The large size of macrovoids enhanced the permeability performance of the membrane, which gave the highest value of PWP and flux.

Then, when the concentration of CTAB was 2.5 wt. % (Figure 31), it resulted in a compressed structure with thicker skin-layer in comparison with the previous

membrane. The pores produced did not interconnected with other pores. At high concentration of the surfactant, in addition to the polymer surfactant complex, free micelles can form with polar groups in the outer layer and non-polar chains inside. These free micelles also results in creation of micro defect in membrane surface (Saedi et al., 2012). This phenomena resulted in decreasing of water and salt permeation of the membrane.

Finally, in the concentration of 3 wt. % of CTAB, the morphology turn into a typical asymmetric channel-like structure as shown in Figure 34. It produced fully develop finger like structure and larger macrovoids formation. This enhanced the performance of membrane in terms of PWP and flux.

(i) Membrane PSP1-C1

FIGURE 29: SEM cross-sectional images of membrane PSP1-C1

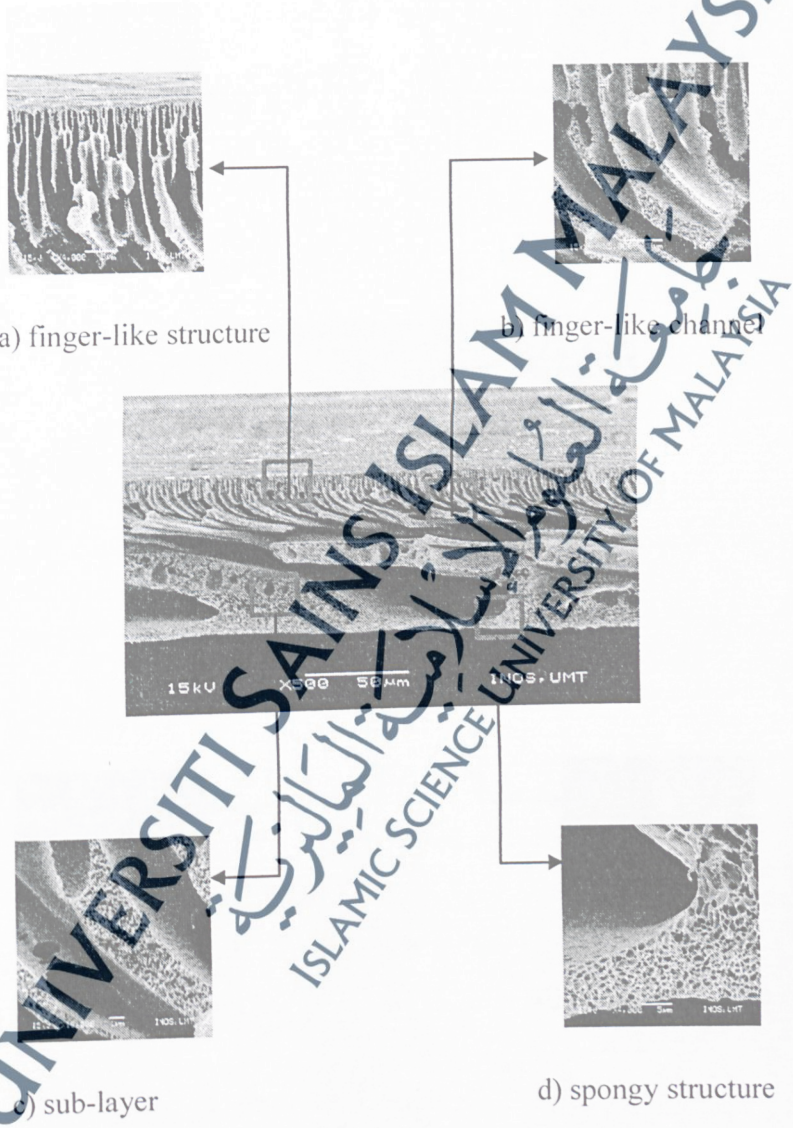

ii) Membrane PSP1-C1.5

FIGURE 30: SEM cross-sectional images of membrane PSP1-C1.5

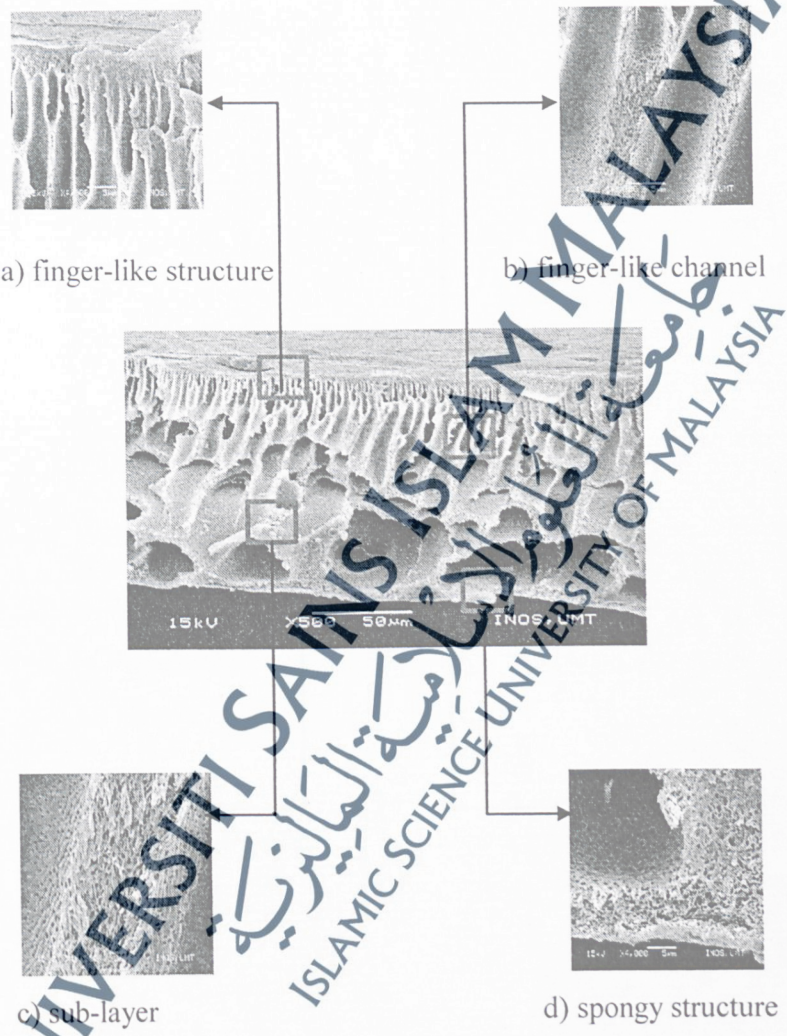

(iii) Membrane PSP1-C2.5

FIGURE 31: SEM cross-sectional images of membrane PSP1-C2.5

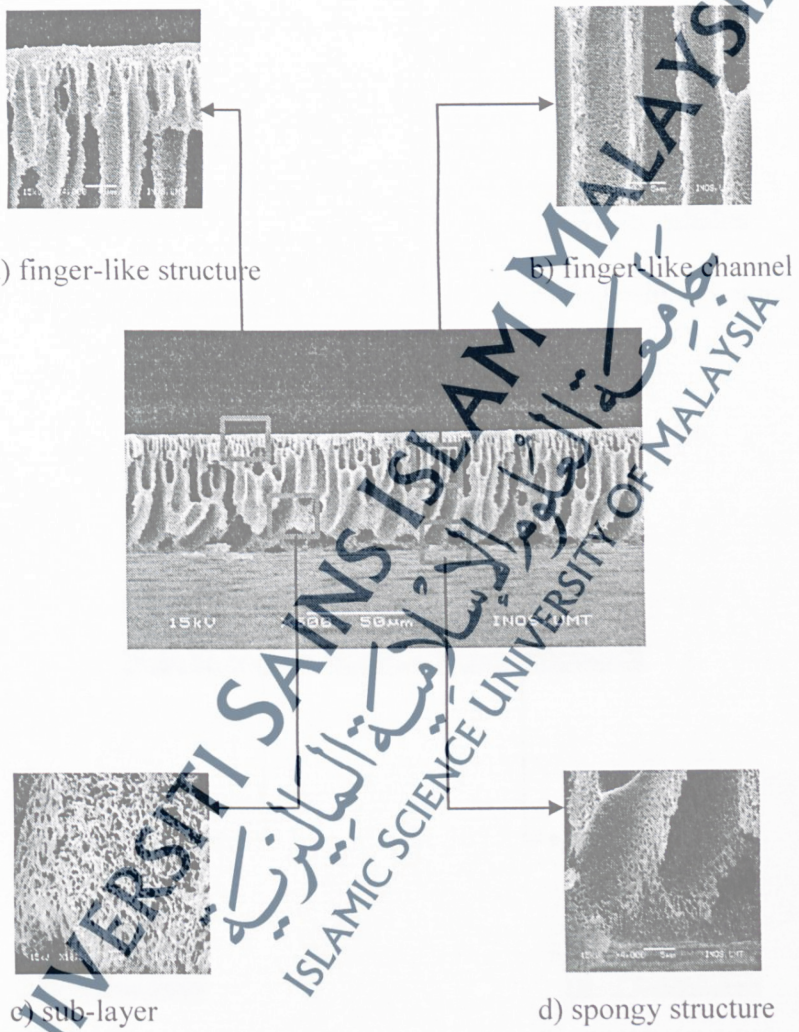

(iv) Membrane PSP1-C3

FIGURE 32: SEM cross-sectional images of membrane PSP1-C3

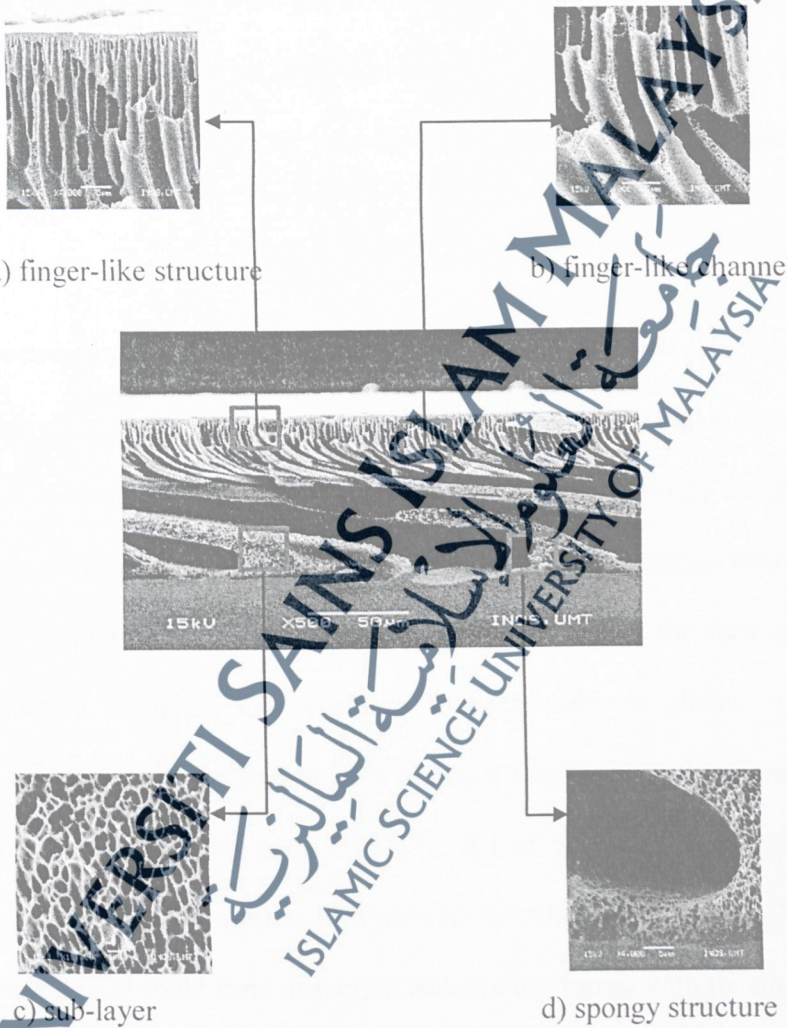

a) finger-like structure

b) finger-like channel

c) sub-layer

d) spongy structure

4.7.4 Effect of Triton X-100 Concentration on Morphology of Membrane

The effect of Triton X-100 concentration on the morphology of membrane have been studied using SEM. The SEM cross sectional images of membranes with different concentration of Triton X-100 were shown in Figure 33 until Figure 36. The thickness of the skin layer decreased for all the membranes in comparison to LPRO membrane without Triton X-100. Moreover, the porosity of the spongy structure of the sub-layer increased as well.

For membrane PSP1-T1 and membrane PSP1-T1.5 as shown in Figure 33 and Figure 34, respectively, the membranes consist of dense top layer and porous sub layer structure. The formation of finger-like pore in the sub layer was fully develop. As the concentration of Triton X-100 increased, the formation of macrovoids become larger. Triton X-100 contains linear alkyl ether chains. Thus, due to the formation of the polymer-surfactant complex, the repulsion between polymer chains is increased resulting in an increase in the free volume and as a result, the higher porosity of the membrane produced. For membrane PSP1-T2, it had been discussed in Figure 25. Meanwhile, at higher concentration of Triton X-100, the ether group in linear alkyl chain of Triton X-100 could form attraction and binding forces with functional groups of the polymer chains. This phenomenon resulted in reduction in the free volume between chains and consequently, leads to the formation of a membrane with compressed structure and less porosity (Rahimpour et al., 2007). This can be clearly seen from the morphological structure of membranes PSP1-T2.5 and membrane PSP1-T3 as shown in Figure 35 and Figure 36, respectively. They produced compact structure with less spongy structure.

(i) Membrane PSP1-T1

FIGURE 33: SEM cross-sectional images of membrane PSP1-T1

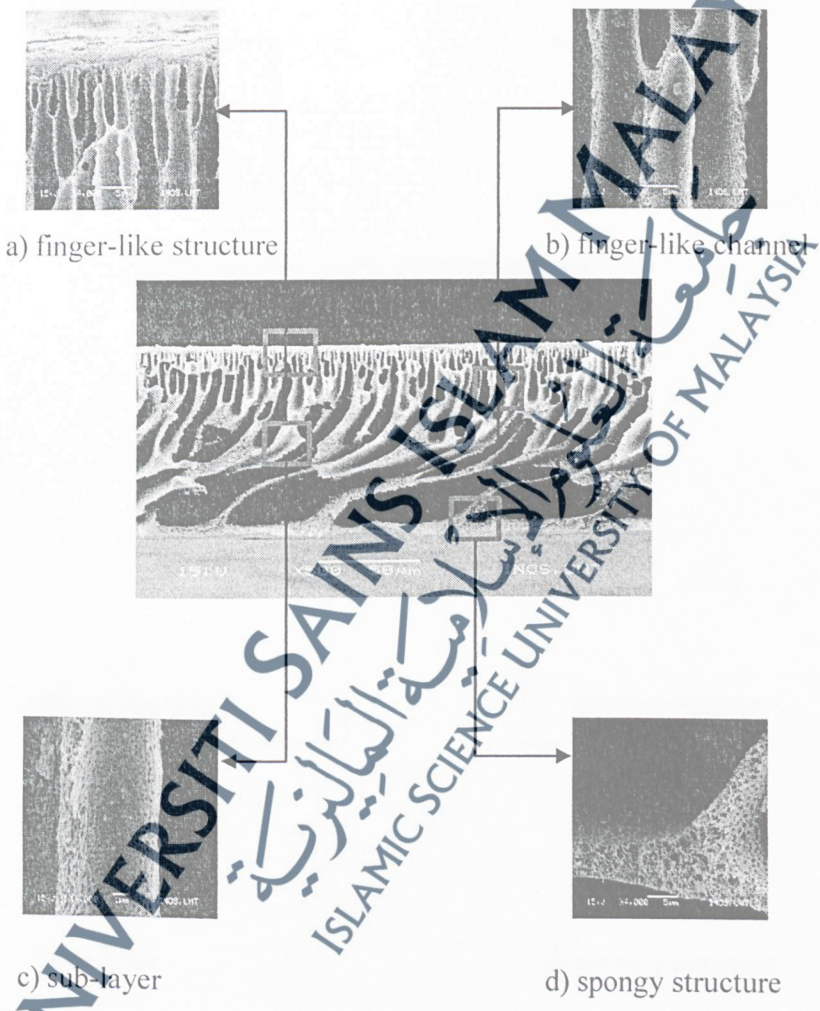

(ii) Membrane PSP1-T1.5

FIGURE 34: SEM cross-sectional images of membrane PSP1-T1.5

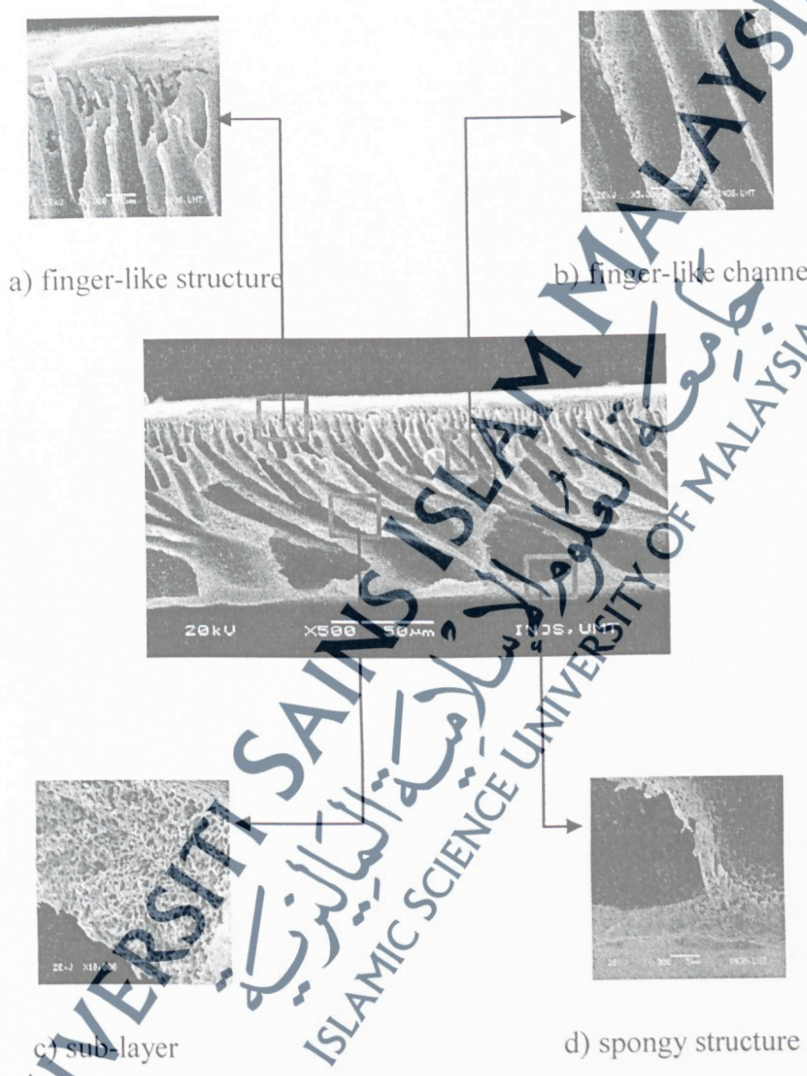

(iii) Membrane PSP1-T2.5

FIGURE 35: SEM cross-sectional images of membrane PSP1-T2.5

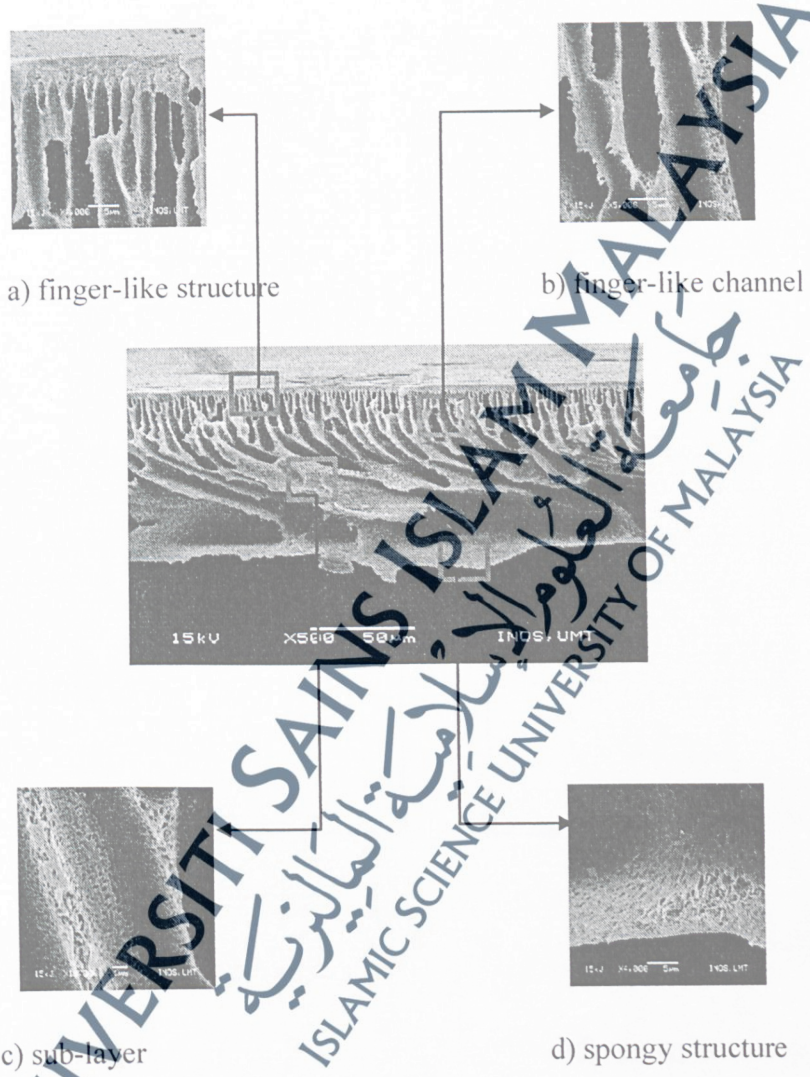

(iv) Membrane PSP1-T3

FIGURE 36: SEM cross-sectional images of membrane PSP1-T3

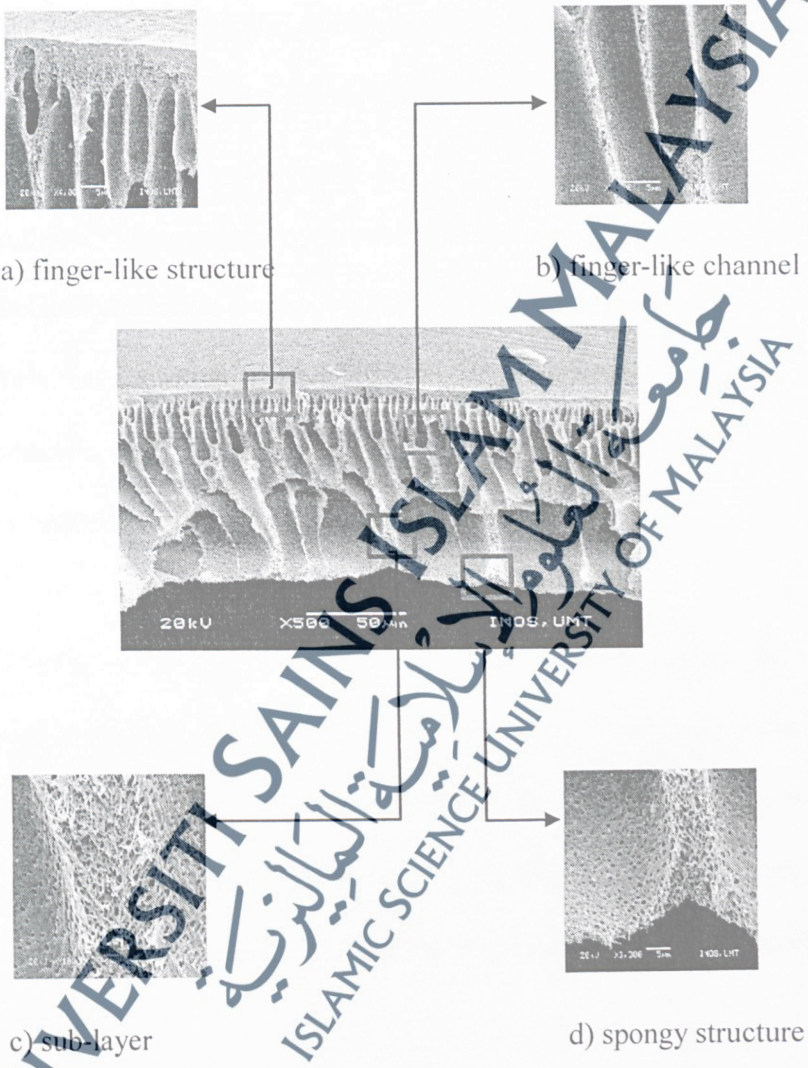

4.7.5 Effect of SDS Concentration on Morphology of Membrane

The SEM images of the cross-sections of the LPRO membrane with different concentration of SDS in the casing solution were shown in Figure 37 until Figure 40. The SEM images indicated that the addition of SDS in the casting solution causes an increase in the formation of macrovoids, depending on the concentration of SDS.

When the SDS concentration introduced to the membrane, which was 1 wt. %, some of its molecule distribute freely in NMP and because of the high concentration of polymer, which was 21 wt. % of PSF, the others could form micelle-like polymer-surfactant complex. Therefore, the macrovoids formation and finger-like structure improved as compared with the membrane without SDS (Figure 37).

Meanwhile, in the presence of 1.5 wt. % SDS concentration, the top layer become thicker and the macrovoids suppressed (Figure 38). This might related with the finding of Saedi et al. (2012) which reported that at higher concentration of SDS, its molecules can form free micelles, and they prefer to form free micelles rather than to form a polymer-surfactant complex, so formation of micelle-like polymer-surfactant complex suppresses.

As the SDS concentration increased up to 2 wt. %, as discussed in (Figure 27) the membrane exhibits characteristic morphology of asymmetric membrane which consist of a dense top layer and porous sub-layer. It produced larger size of macrovoids as compared with membrane with other SDS concentration, hence improve and gave the highest value for the permeability performance of the membrane.

For membrane with 2.5 and 3.0 wt. % of SDS, both of them exhibited denser top layer and fully develop finger-like structure in sub layer of membrane as shown in Figure 39 and Figure 40. Number of pores produced increased as compared with membrane of lower concentration of SDS. The spongy structure gradually become compact. It reduced the porosity of membrane support layer and resulted in lower PWP and salt performance.

(i) Membrane PSP1-S1

FIGURE 37: SEM cross-sectional images of membrane PSP1-S1

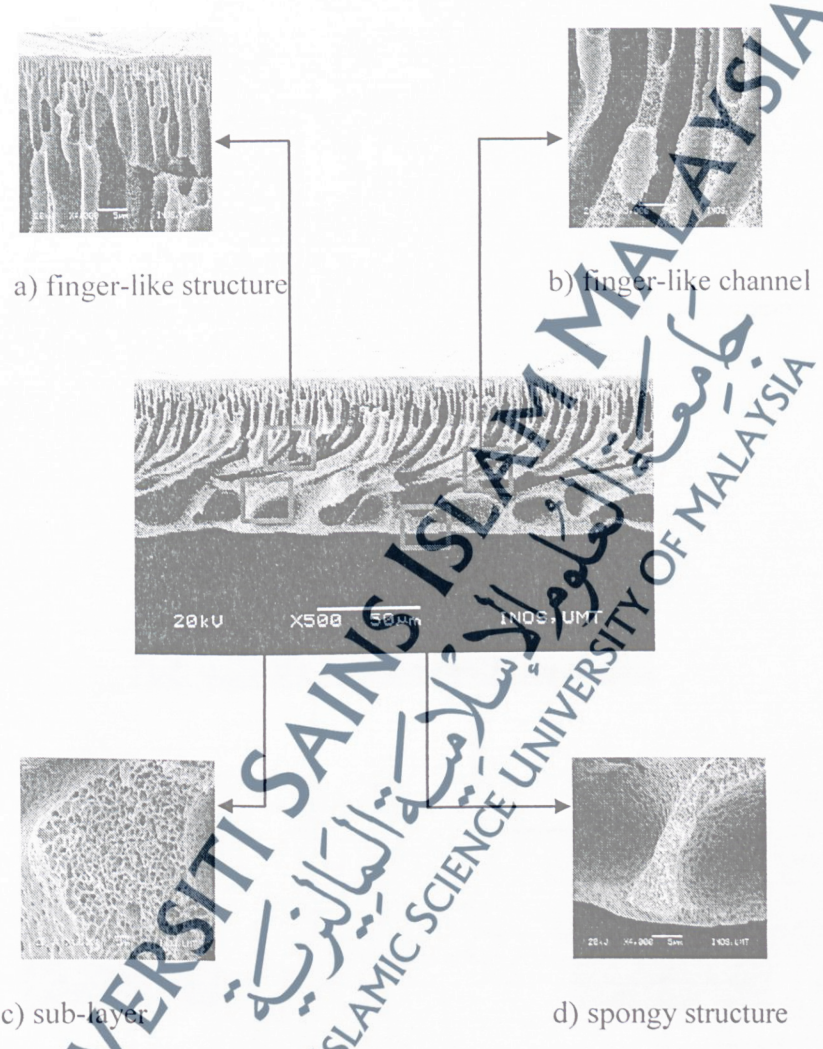

(ii) Membrane PSP1-S1.5

FIGURE 38: SEM cross-sectional images of membrane PSP1-S1.5

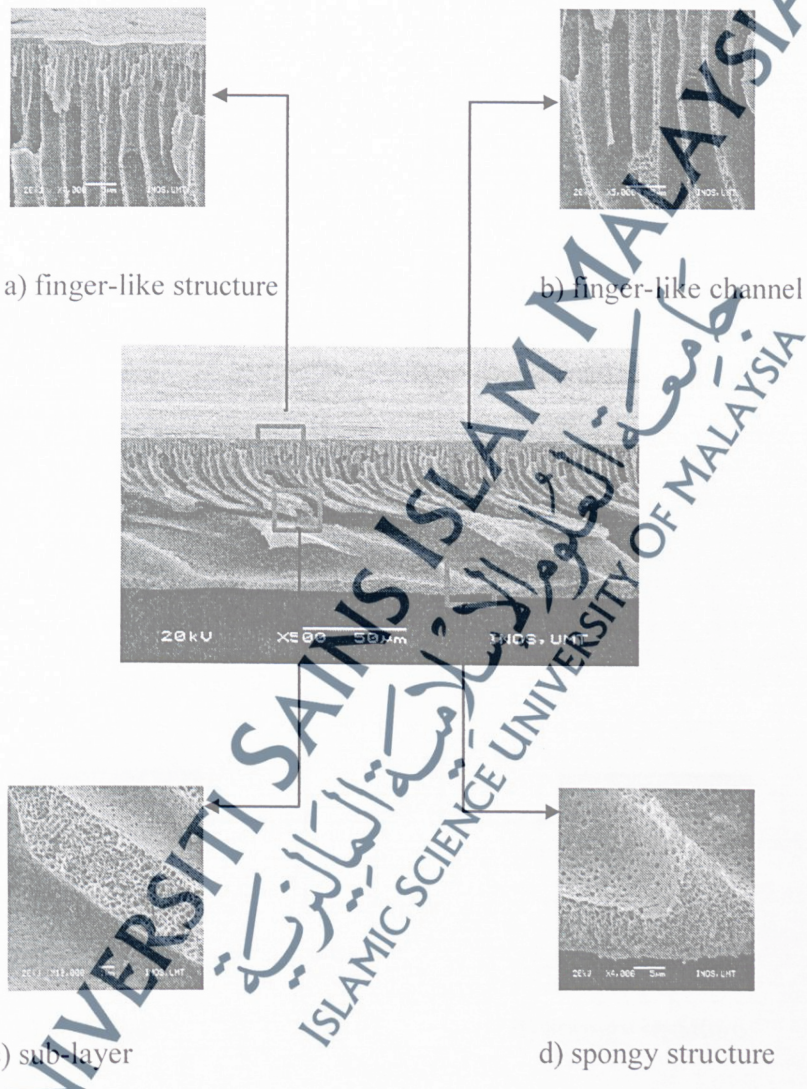

(iii) Membrane PSP1-S2.5

FIGURE 39: SEM cross-sectional images of membrane PSP1-S2.5

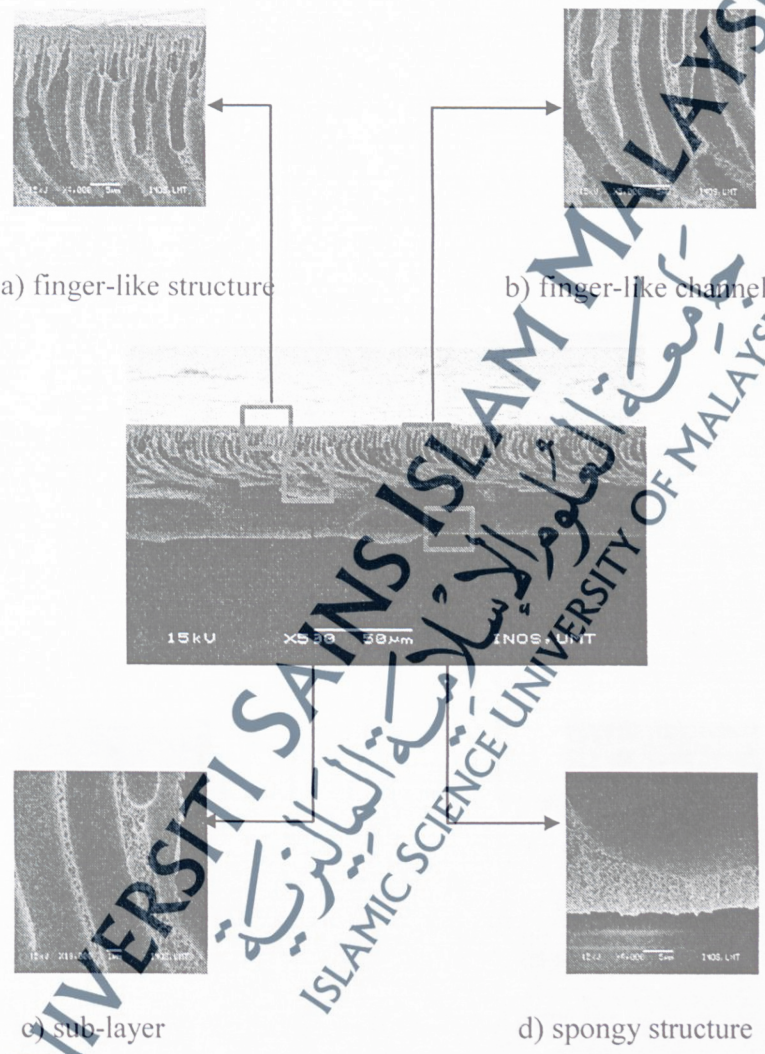

(v) Membrane PSP1-S3

FIGURE 40: SEM cross-sectional images of membrane PSP1-S3

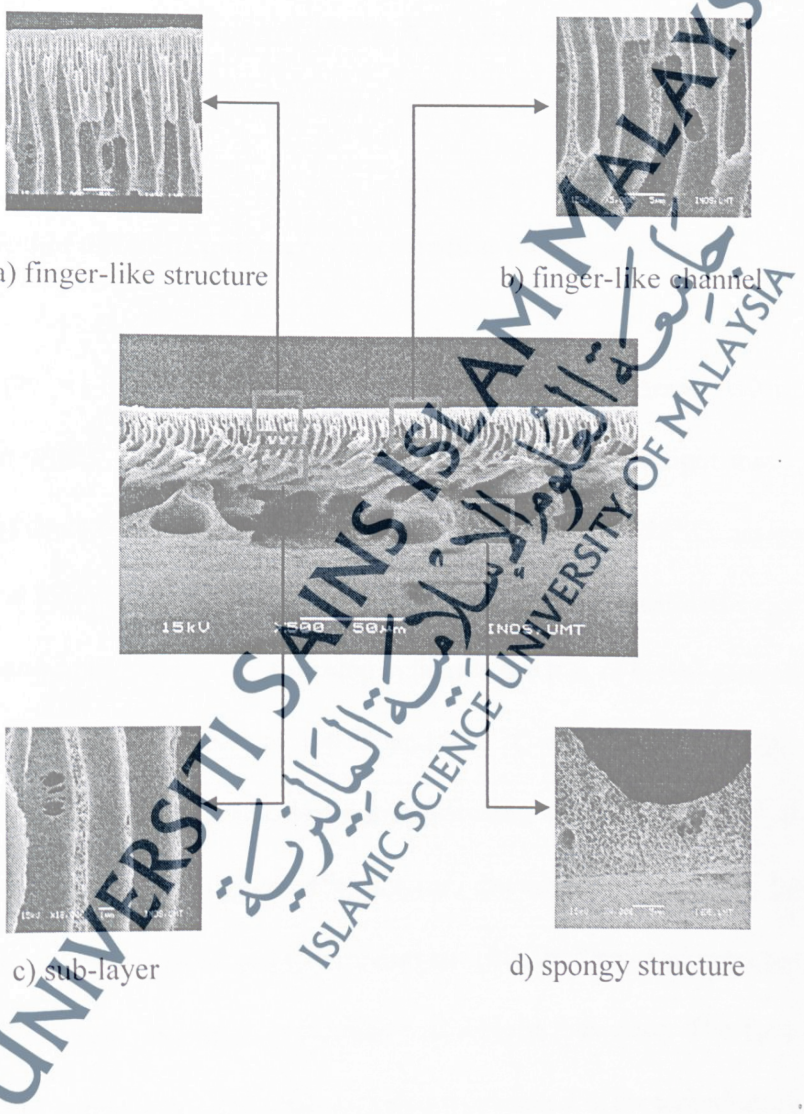

4.8 Thermal Study using Thermal Gravimetric Analysis (TGA)

The thermal study was carried out to examine the thermal stability of the prepared membranes. The analysis were performed using Mettler Toledo TGA/DSC apparatus in the temperature range of 30-800 ^{0}C under dynamic nitrogen atmosphere at a heating rate of 10 ^{0}C min^{-1} with 20 ml/min of flow rate.

4.8.1 Effect of different polymer concentration on thermal study

Figure 41 showed the TGA curve for the membrane with different concentration of PSF polymer. For PSP1, it exhibit single step weight loss only. The weight loss of about 68 % in a temperature range of 358 ^{0}C and 688 ^{0}C, assigned to the degradation of PSF polymer main chain (Devrim et al, 2009). Meanwhile, for PSP3, it showed two weight loss steps. The first step indicated the loss of bound water and traces of solvent in a temperature range of 360 ^{0}C and 480 ^{0}C with the total weight loss of 6 %. Then, for the second step, at the temperature between 480 ^{0}C and 711 ^{0}C, the weight loss observed of about 56 % suggested the polymer degradation. This result fairly agree with the finding of Venugopal and Dharmalingam (2012). They had reported the PSF is highly thermal stable polymer, it exhibits two weight loss steps. The first step that indicated loss of bound water and traces of solvent occurred in the temperature range of 270 ^{0}C to 490 ^{0}C. Then, the steep loss in weight observed beyond this temperature suggested that beyond 490 ^{0}C, the polymer degraded.

FIGURE 41: TGA curve for RO membrane with different PSF concentration

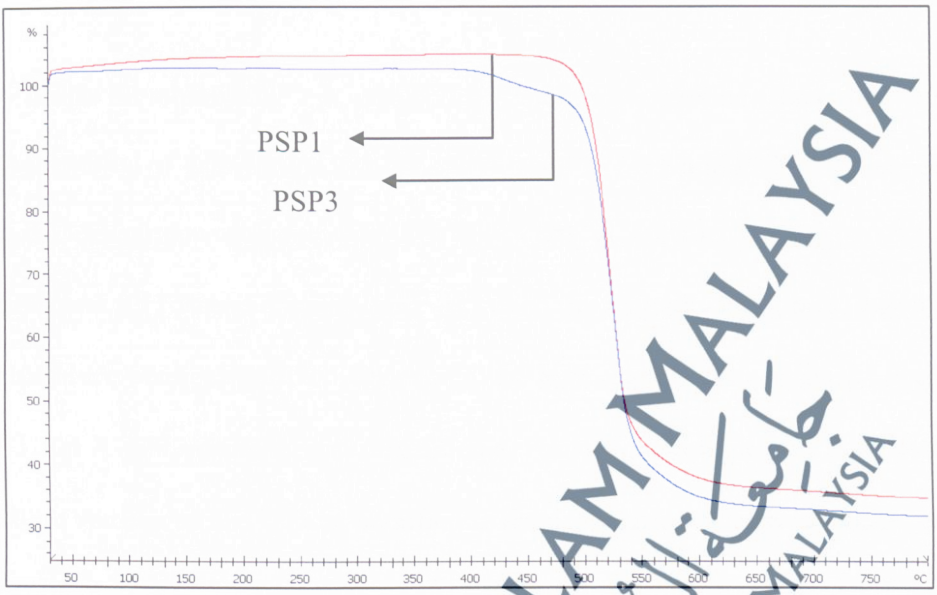

4.8.2 Effect of different polymer concentration with surfactant on thermal study.

TGA curve for membrane of different PSF concentration with surfactant was demonstrated in Figure 42. For both membrane PSP1-C2 and PSP3-C2, they showed a three step weight loss. The first weight loss was observed between 80 ^{0}C and 150 ^{0}C for PSP1-C2 and between 130 ^{0}C and 250 ^{0}C for PSP3-C2 which may due to removal of physically and chemically bonded water along with trace amounts of solvents. The presence of water was due to the hydrophilic nature of membrane and the solvent which was used for casting (Venugopal and Dharmalingam, 2012). The second weight loss between 400 ^{0}C and 480 ^{0}C for membrane PSP1-C2 and 380 ^{0}C and 510 ^{0}C for membrane PSP3-C2 may due to degradation of the CTAB group while the third weight loss that occurred beyond 520 ^{0}C for both membrane were attributed to the main

degradation of polymer with the residual percentages of 48.2 % (PSP1-C2) and 33.7% (PSP3-C2).

Meanwhile for membrane PSP1-T2 and PSP3-T2, they also exhibits a three steps weight loss. The removal of water and traces for membrane PSP1-T2 and PSP3-T2 were found to be at the temperature range from 120 ^{0}C until 280 ^{0}C and 140 ^{0}C until 220 ^{0}C with the weight loss of 1 % and 3%, respectively. Then, the second weight loss observed at the temperature between 350 ^{0}C and 480 ^{0}C for both membrane was assigned to the loss of Trion X-100 molecule in the membrane. For both membrane, the third thermal degradation starting at 500 ^{0}C was signified to the degradation of polymer main chain.

TGA graphs for membranes PSP1-S2 and PSP3-2 also observed three stages degradation. The first weight loss were observed between 150 ^{0}C – 300 ^{0}C (PSP1-S2) and 50 ^{0}C – 270 ^{0}C (PSP3-S2) can be due to the removal of water and solvent traces. The second loss occurred around 350 ^{0}C to 450 ^{0}C for both membranes were related to the loss of SDS molecule in the membrane, while the third weight loss that occurred beyond 490 ^{0}C was attributed to the main chain of polymer degradation with the residual percentages of 39.4 % (PSP1-S2) and 42.4 % (PSP3-S2).

FIGURE 42: TGA curve for RO membrane of different PSF concentration with surfactant

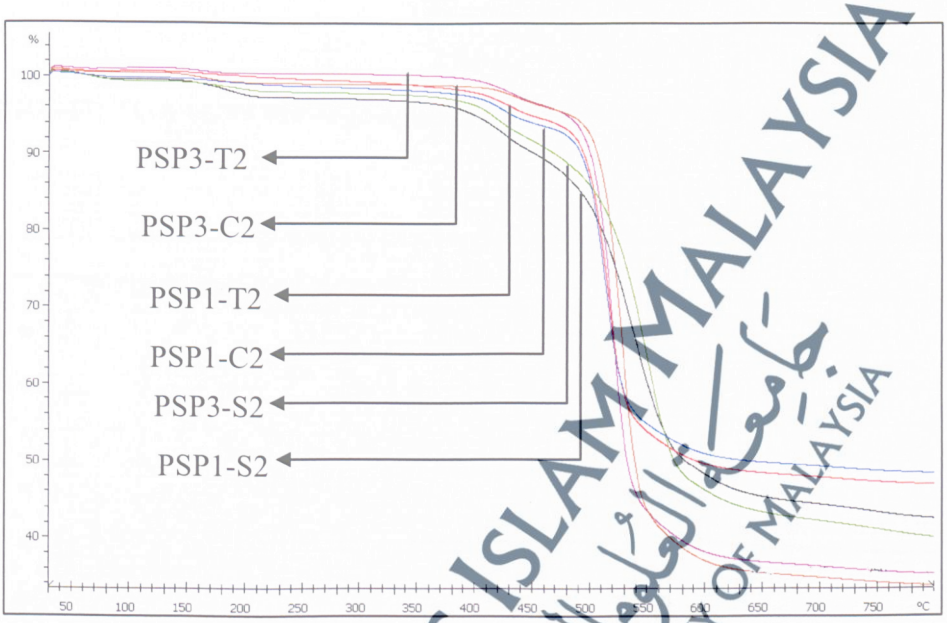

4.8.3 Effect of CTAB concentration on thermal study

Figure 43 illustrated the TGA curve of PSF membrane with different concentration of CTAB which varied from 1.0 wt. % until 3. 0 wt. %. Generally, for all the five membrane, they exhibits a three step weight loss. The first step indicated the dehydration of physically and chemically adsorbed water and removal of solvent traces. This step can be observed in the temperature range of 40 ^{0}C and 240 ^{0}C for all five membranes with the weight loss of 1 %, except for PSP1-C3 which is 3 %. The second weight loss observed at the temperature between 400 ^{0}C and 480 ^{0}C for all the membranes may due to the decomposition of CTAB as surfactant, with the weight loss around 6%. Then, for the third weight loss that occurred beyond the temperature of 500

^{0}C were attributed to the main chain of polymer degradation, with the residual percentages of 53.5 % (PSP1-C1), 47.7 % (PSP1-C1.5), 48.2% (PSP1-C2), 51.4 % (PSP1-C2.5), and 9.8 % (PSP1-C3).

FIGURE 43: TGA curve of RO membrane with different CTAB concentration

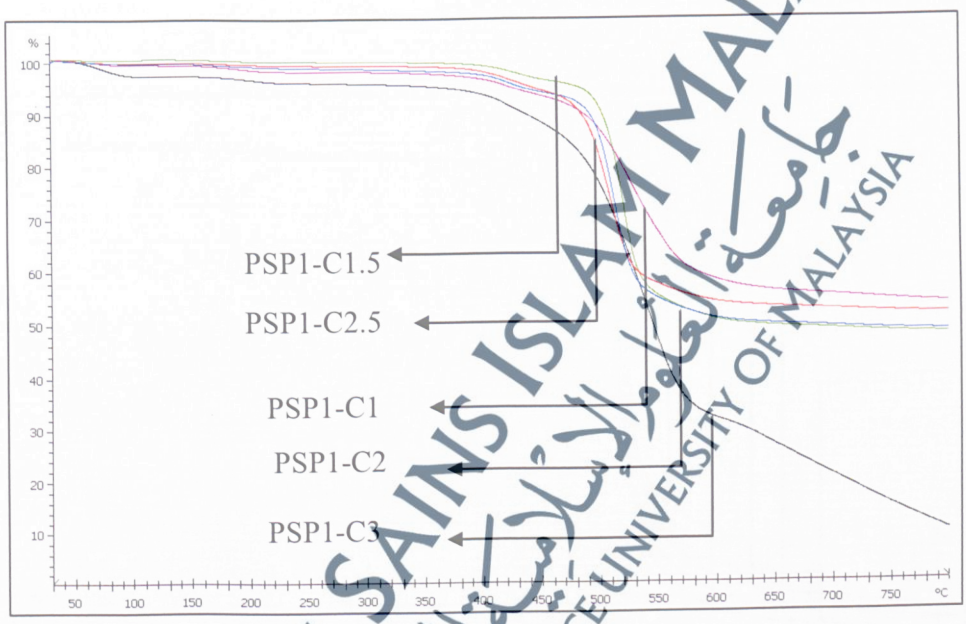

4.8.4 Effect of Triton X-100 concentration on thermal study

TGA curve of membrane with different Triton X-100 concentration was shown in Figure 44. It also observed a three steps weight loss for all the five membranes. For the first weight loss, the removal of water and traces were found to be at the temperature of 150 ^{0}C and 270 ^{0}C, with the weight loss of about 1% for all samples. Then, the second weight loss of about 5% occurring in between the temperature of 390 ^{0}C and 480 ^{0}C were related to the removal of Triton X-100 group from the membranes.

Meanwhile, for the third thermal degradation, it started at 500 ^{0}C and was assigned to the degradation of polymer main chain with the residual percentages for PSP1-T1, PSP1-T1.5, PSP1-T2, PSP1-T2.5 and PSP1-T3 are 48 %, 53.5 %, 46.8 %, 50.8 % and 45 %, respectively.

FIGURE 44: TGA curve of RO membrane with different Triton X-100 concentration

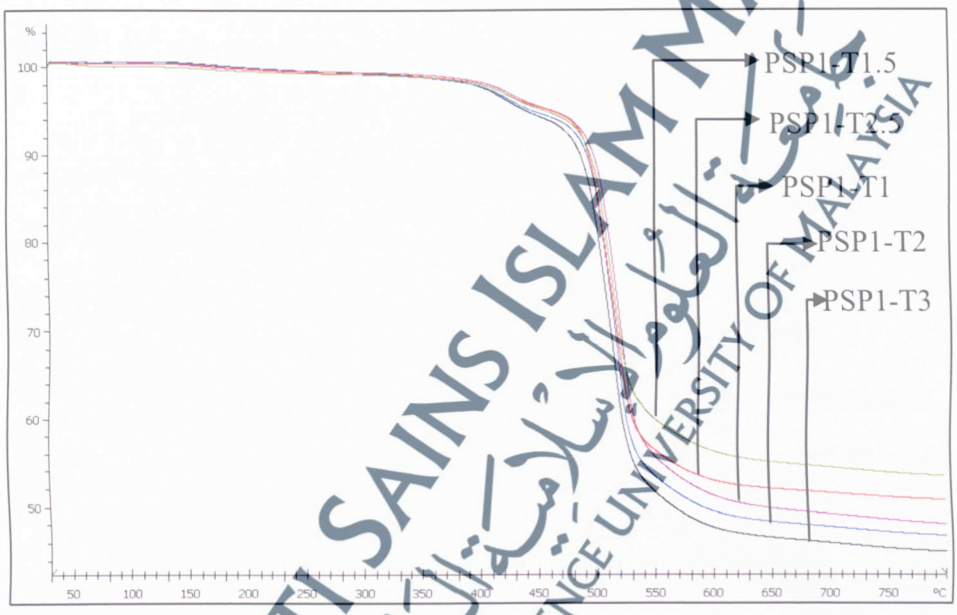

4.8.5 Effect of SDS concentration on thermal study

In the case of different SDS concentration, as depicted in Figure 45, the degradation occurred in three steps. The first step indicated the removal of physically and chemically bonded water along with trace amounts of solvents in a temperature range of 150 ^{0}C and 300 ^{0}C with the total weight loss of 1 % for membranes PSP1-S1, PSP1-S1.5, and PSP1-S3, while for PSP1-S2 and PSP1-S2.5, the weight loss was about

2 %. The second gradual degradation from 380 ^{0}C to 480 ^{0}C was assigned to the loss of SDS group from the membranes. The weight loss was recorded of about 8 % for all membranes, except for PSP1-S1 which is 6 %. Then, the third weight loss that occurred beyond 500 ^{0}C were attributed to the main degradation of polymer, with the residual percentages of PSP1-S1, PSP1-S1.5, PSP1-S2, PSP1-S2.5 and PSP1-S3 are 21.3 %, 30.7 %, 39.4 %, 32.3% and 38.4%, respectively.

FIGURE 45: TGA curve of RO membrane with different SDS concentration

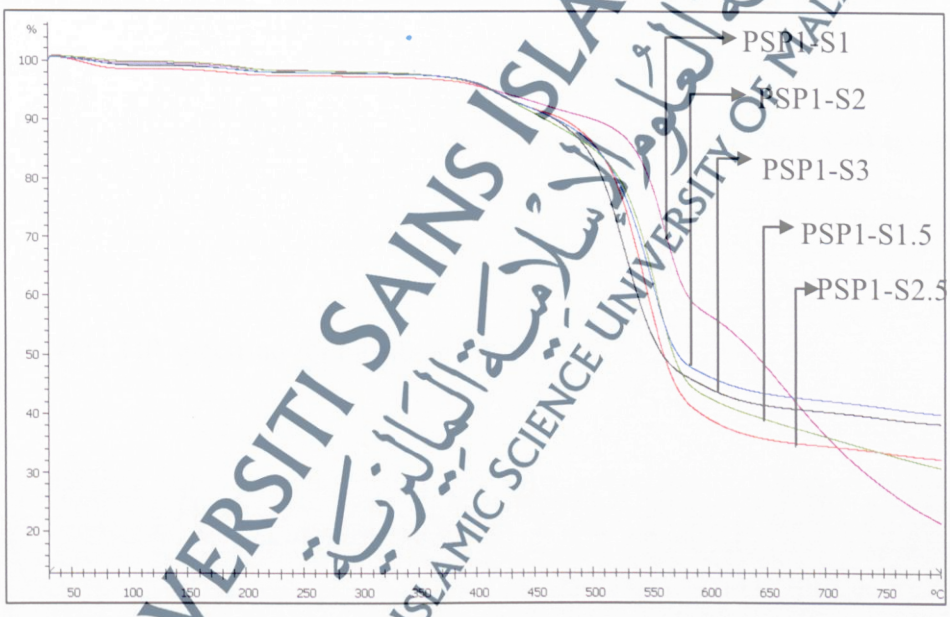

4.9 Physico-chemical Study using Fourier Transform Infrared (FTIR)

FTIR was employed as a technique to reveal some kind of information regarding intermolecular interaction between the molecules in the membrane. FTIR plays a decisive role in order to obtain knowledge about the existing functional groups

within the molecules. The existing structural changes are interpreted in terms of frequency or band shift (Krzaczkowska et al., 2006).

1) Membrane PSP1

From the spectrum of membrane PSP1 (Figure 46), the transmittance band observed near 3412 cm^{-1} was assigned to O-H stretching vibration of PSF polymer. The presence of aromatic C=C bond which belong to PSF polymer was interpreted at 1585 cm^{-1}. In addition, the transmittance band observed at 1490 can be explained owing to the C-N bond stretching vibration. Presence of C-N band in this spectrum proved that the presence of PVP as additive in the membrane formulation. Moreover, strong peaks observed at 1243 and 1151 were ascribed to the existence of C=O and S=O bonds in PSF, respectively.

FIGURE 46: FTIR spectrum for membrane PSP1

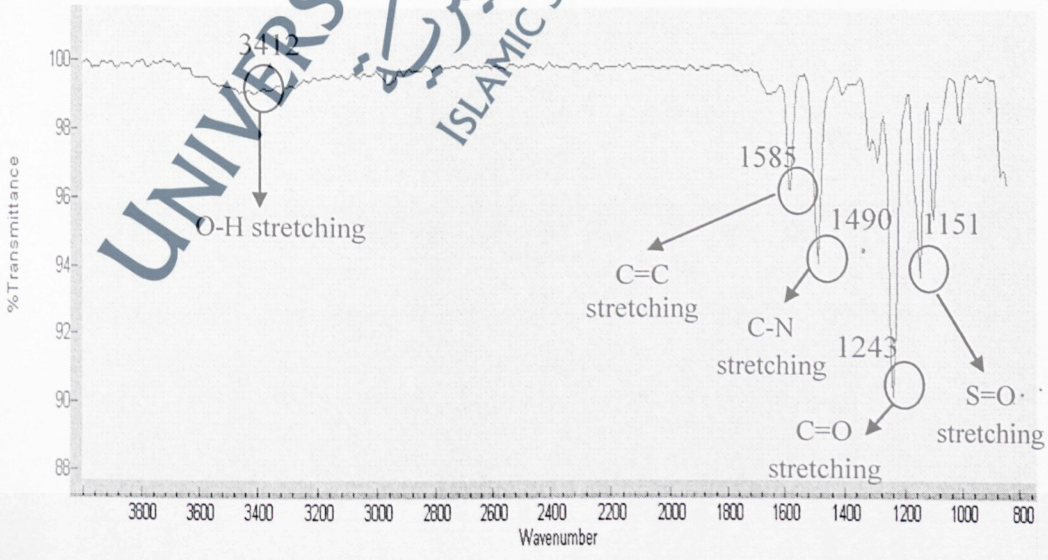

2) Membrane PSP3

Figure 47 demonstrated the FTIR spectrum for membrane PSP3. The strong peaks observed at 1585 cm^{-1}, 1490 $cm^{-1}$and 1243 cm^{-1}, which belong to C=C stretching, C-N stretching and C=O stretching, respectively were similar for those obtained in the spectrum of membrane PSP1. On the other hand, the O-H stretching vibration of PSF polymer was shifted from 3412 cm^{-1} to 3485 cm^{-1}. Meanwhile, the intense peak observed at 1152 cm^{-1} assigned to the S=O stretching which is slightly shifted as compared to the peak in membrane PSP1.

FIGURE 47: FTIR spectrum for membrane PSP3

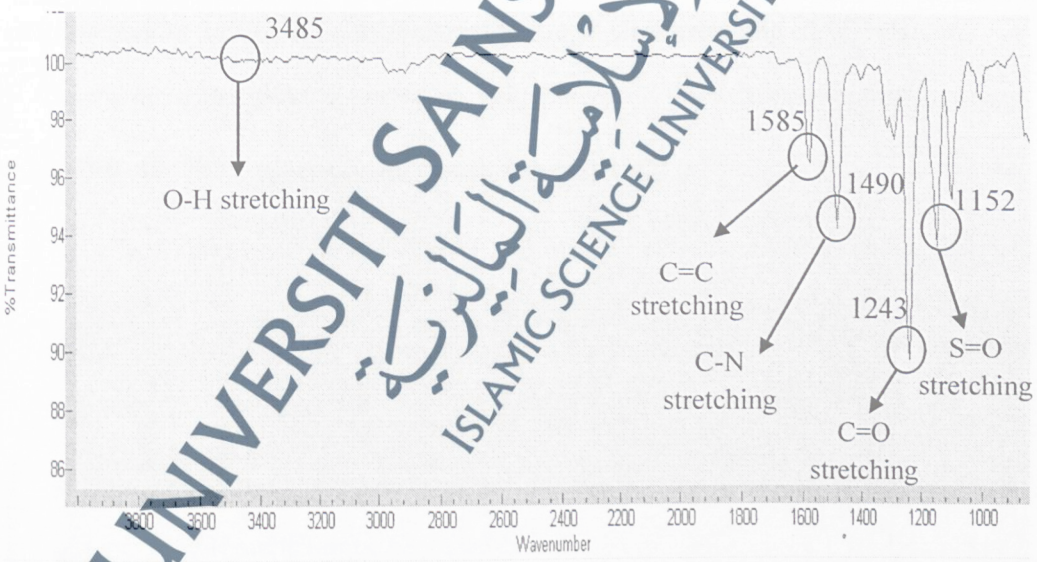

3) Membrane PSP1-C2.0

FTIR spectrum for membrane PSP1-C2.0 wasshown in Figure 48. The addition of CTAB in the casting solution gave slight changes in the spectrum of membrane. For O-H stretching vibration, it was shifted to 3454 cm^{-1} compared to membrane PSP1 (3412 cm^{-1}). Strong peaks that observed at 1585 cm^{-1}, 1490 cm^{-1}, 1243 cm^{-1} and 1151 cm^{-1} were ascribed to the existence of C=C stretching, C-N stretching, C=O stretching and S=O stretching, respectively. The addition of CTAB does not affect those functional group as they exhibit the same wavenumber as found in membrane PSP1. Instead, the significant transmittance band observed at 1410 cm^{-1} was assigned to N-CH_3 stretching. The N-CH_3 group belongs to CTAB, thus reveal the presence of CTAB in the membrane formulation. This was correspond to the study by Viana et al., (2012), which reported that the peak at 1480 cm^{-1} was assigned to the N-CH_3 stretching of CTAB.

FIGURE 48: FTIR spectrum for membrane PSP1-C2.0

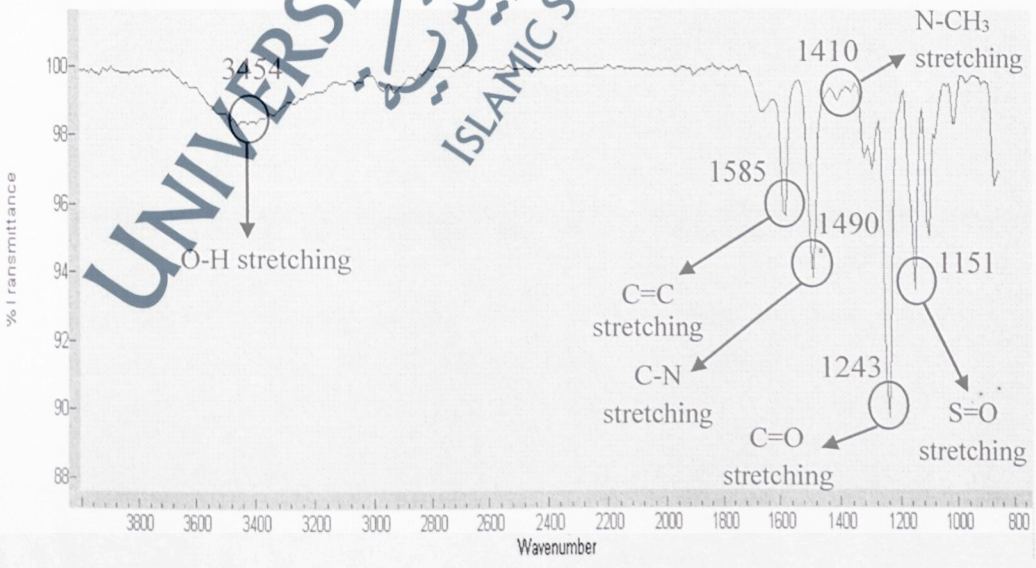

4) Membrane PSP3-C2.0

Figure 49 depicted the FTIR spectrum for membrane PSP-C2.0. The appearance of peak at 1409 cm^{-1} in the spectrum confirmed the presence of N-CH_3, which was the characteristic peak for CTAB. The presence of O-H stretching vibration interpreted at the transmittance band of 3464 cm^{-1}. The C=C stretching, C-N stretching, C=O stretching and S=O stretching were recorded at 1585 cm^{-1}, 1490 cm^{-1}, 1243 cm^{-1} and 1151 cm^{-1}, respectively which were almost the same as those obtained in membrane PSP3.

FIGURE 49: FTIR spectrum for membrane PSP3-C2.0

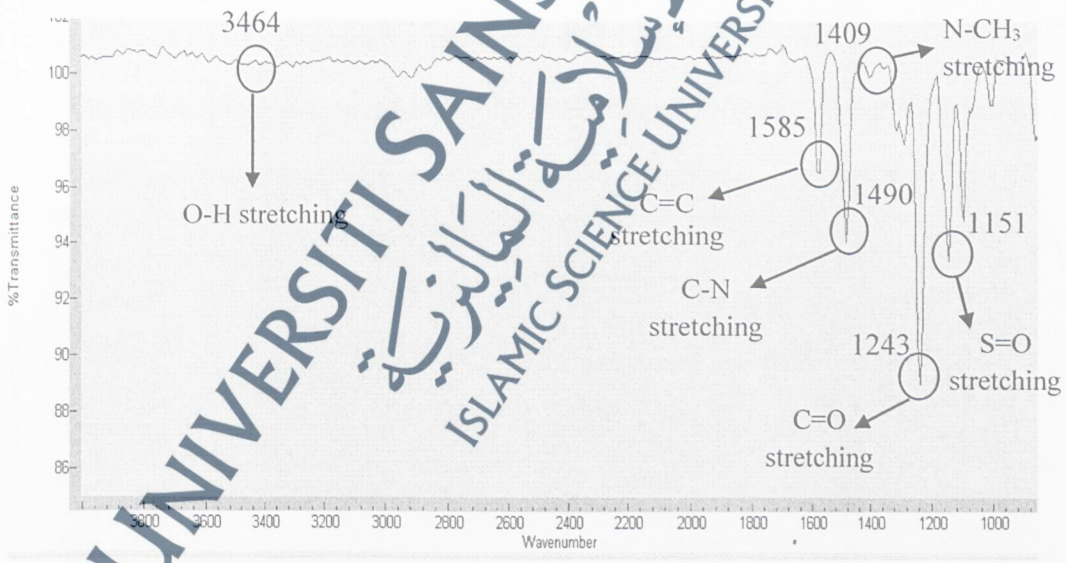

5) Membrane PSP1-T2.0

From FTIR spectrum for membrane PSP1-T2.0 (Figure 50), the transmittance band observed near 3449 cm^{-1} was attributed to the presence of O-H bond of PSF polymer. Strong peaks observed at 1584 cm^{-1}, 1489 cm^{-1}, 1243 cm^{-1} and 1151 cm^{-1} were ascribed to the existence of C=C stretching, C-N stretching, C=O stretching and S=O stretching, respectively. These peaks were nearly the same as compared to membrane PSP1. On the other hand, the important peak had been observed at 1106 cm^{-1} which assigned to the C-O stretching, revealed the presence of Triton X-100 in the membrane solution. This peak agreed with the finding of Kimura et al., (1996) which found the C-O stretching of Triton X-100 at 1099 cm^{-1}.

FIGURE 50: FTIR spectrum for membrane PSP1-T2.0

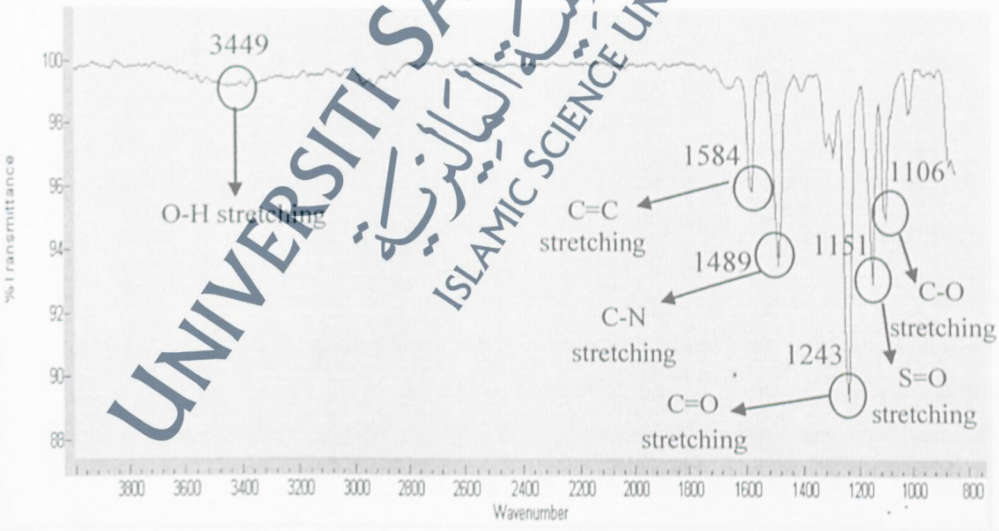

6) Membrane PSP3-T2.0

Figure 51 demonstrated the FTIR spectrum for membrane PSP3-T2.0. The O-H group of PSF showed a broad peak at 3484 cm^{-1} which was slightly shifted from membrane PSP1-T2.0 (3449 cm^{-1}). For C=C stretching and C-N stretching, the strong peaks observed almost similar to those obtained in membrane PSP1-T2.0 which were at 1585 cm^{-1} and 1490 cm^{-1}, respectively. Addition of Triton X-100 does not change the peak for C=O stretching and S=O stretching in membrane PSP3-T2 as it gave the same value of wavenumber in membrane PSP3. Similar to PSP1-T2.0, the existence of Triton X-100 in the membrane formulation confirmed by the interpretation of strong peak at 1106 cm^{-1} which belong to the C-O group of Triton X-100.

FIGURE 51: FTIR spectrum for membrane PSP3-T2.0

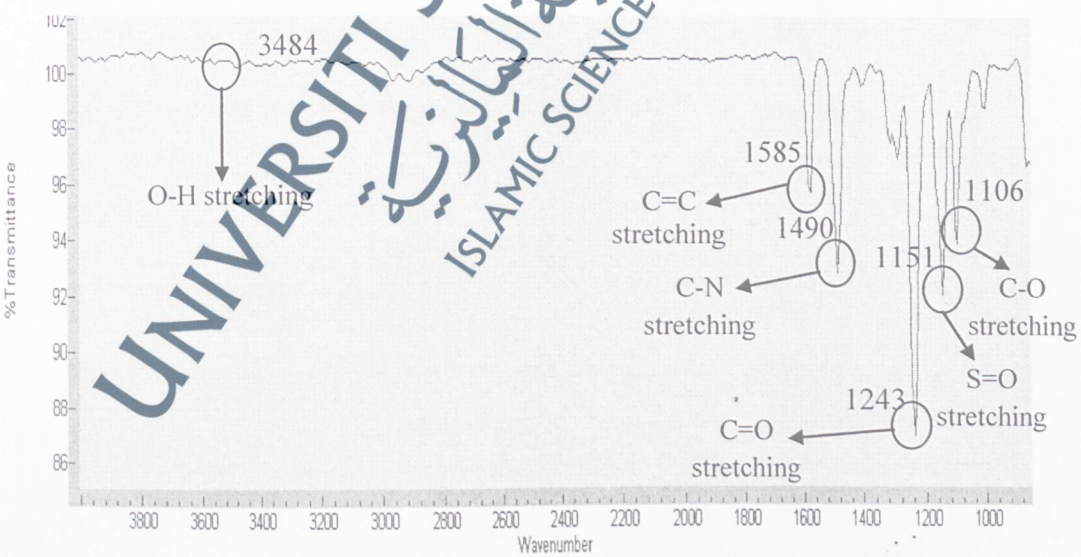

7) Membrane PSP1-S2.0

FTIR spectrum for membrane PSP1-S2.0 was shown in Figure 52. The addition of small amount of SDS in the casting solution affected the spectrum of membrane. For O-H stretching vibration, it was shifted to 3440 cm^{-1} by comparing with membrane PSP1 which is at 3412 cm^{-1} of wavenumber. The C=C stretching, C=O stretching and S=O stretching of PSF polymer were interpreted at 1580 cm^{-1}, 1243 cm^{-1}, and 1152 cm^{-1}, respectively which were slightly shifted from those obtained in membrane PSP1. Addition of SDS does not change the peak for C-N stretching in membrane PSP1-S2 as it gave the same value of wavenumber in membrane PSP1 which is at 1486 cm^{-1}. On the other hand, a significant peak had been observed at 2864 cm^{-1} which assigned to the C-H_3 stretching, confirmed the existence of SDS molecule in the membrane solution. This peak in line with the finding of Viana et al., (2012) which discover the stretching of C-H_3 group from SDS at 2873 cm^{-1}.

FIGURE 52: FTIR spectrum for membrane PSP1-S2.0

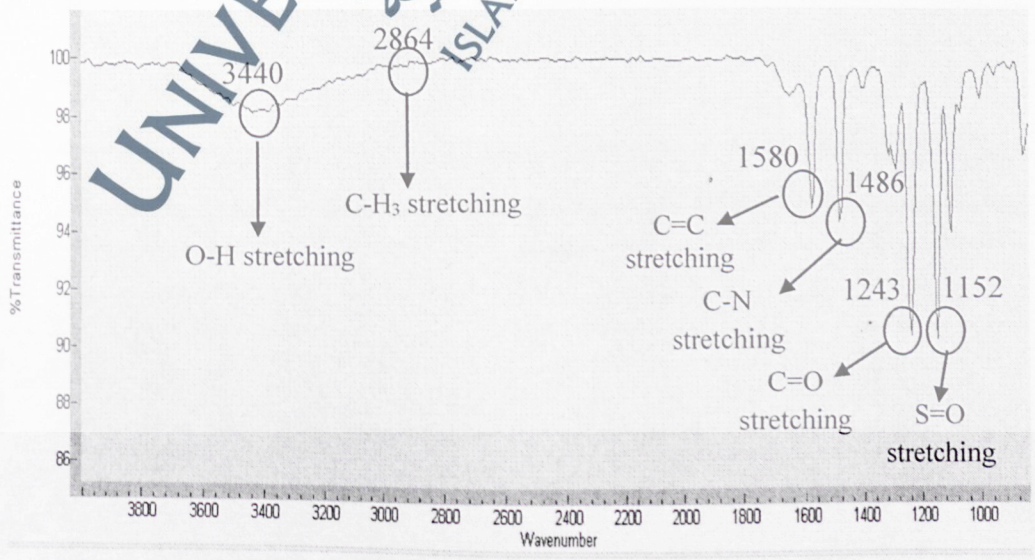

8) Membrane PSP3-S2.0

From FTIR spectrum for membrane PSP3-S2.0 (Figure 53), the transmittance band observed near 3464 cm^{-1} was attributed to the presence of O-H bond of PSF polymer. The appearance of peak at 2919 cm^{-1} in the spectrum revealed the presence of $C-H_3$ group, which was the important peak for SDS. It is slightly shifted from membrane PSP1-S2.0 which is at 2864 cm^{-1}. The intense peaks observed at 1578 cm^{-1}, 1484 cm^{-1}, 1242 cm^{-1} and 1154 cm^{-1} were ascribed to the existence of C=C stretching, C-N stretching, C=O stretching and S=O stretching, respectively. It shows that addition of small amount of SDS contribute the small effect to the spectrum of membrane.

FIGURE 53: FTIR spectrum for membrane PSP3-S2.0

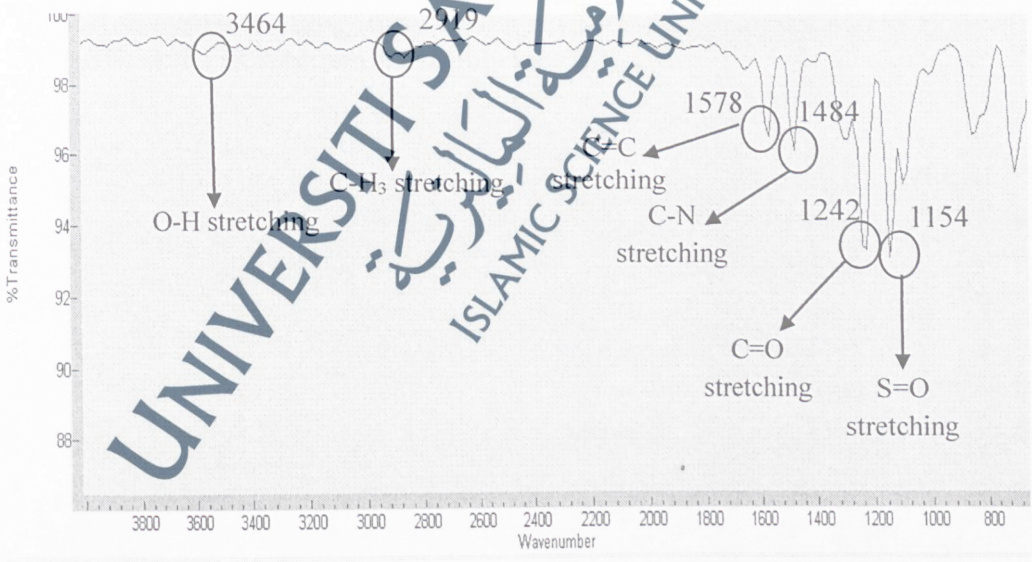

9) Membrane PSP1-C1

Figure 54 showed the FTIR spectrum for membrane PSP1-C1. Similar to the membrane PSP1-C2.0 that had been described previously, addition of small amount of CTAB slightly change the spectrum of the membrane. In this spectrum, the O-H stretching for PSF polymer was interpreted at the wavenumber of 3439 cm^{-1}, shifted to the left from those found in pure PSF membrane (PSP1) which is 3412 cm^{-1}. The existence of CTAB molecule in the membrane proven by the strong peak at 1407 cm^{-1} represent the N-CH_3 group from CTAB. The C=C stretching, C-N stretching, C=O stretching and S=O stretching of PSF polymer were interpreted at 1579 cm^{-1}, 1484 cm^{-1}, 1242 cm^{-1}, and 1151 cm^{-1}, respectively which are slightly shifted from those obtained in membrane PSP1.

FIGURE 54: FTIR spectrum for membrane PSP1-C1.0

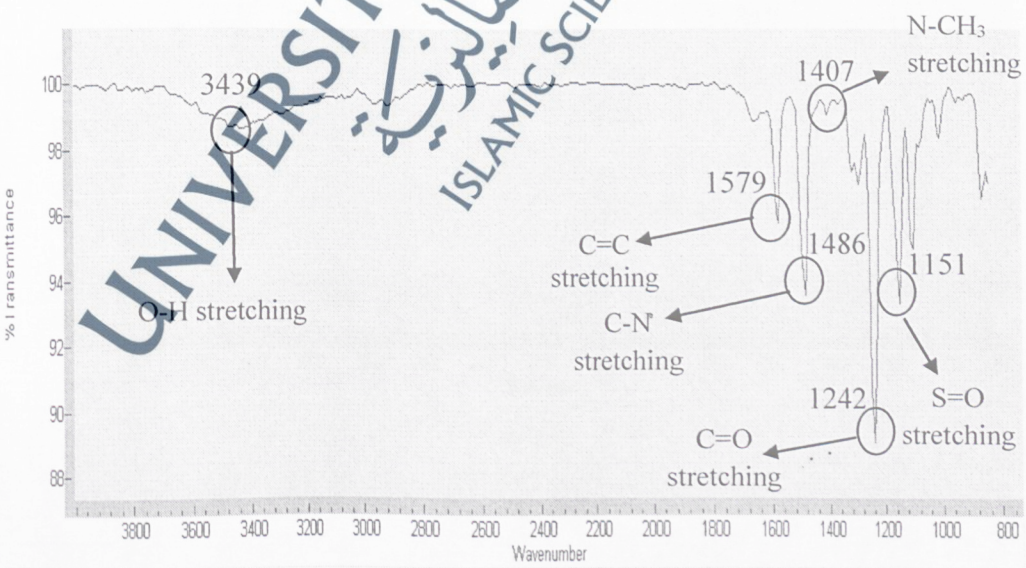

10) Membrane PSP1-C1.5

Figure 55 demonstrated the FTIR spectrum for membrane PSP1-C1.5. The O-H group of PSF shows a broad peak at 3432 cm^{-1} which was slightly shifted from membrane PSP1 (3412 cm^{-1}). For C=C stretching, C-N stretching, C=O stretching and S=O stretching, the strong peaks observed almost similar to those obtained in membrane PSP1 which are at 1584 cm^{-1} , 1490 cm^{-1}, 1242 cm^{-1} and 1151 cm^{-1}, respectively. Increasing of CTAB concentration does not affects the spectrum of the membrane as it exhibits the strong peak at 1408 cm^{-1} represented $N-CH_3$ group in CTAB, which was almost similar for those obtained in membrane PSP1-C1.0.

FIGURE 55: FTIR spectrum for membrane PSP1-C1.5

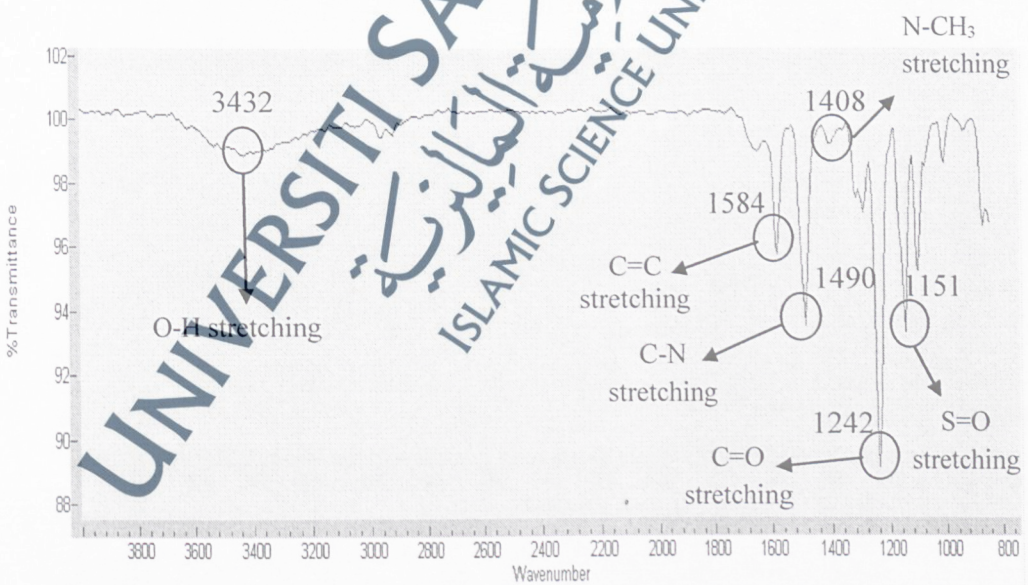

11) Membrane PSP1-C2.5

FTIR spectrum for membrane PSP1-C2.5 had been illustrated in Figure 56. For O-H stretching vibration, it was shifted to 3436 cm^{-1} by comparing with membrane PSP1 which is at 3412 cm^{-1} of wavenumber. As the concentration of CTAB increased up to 2.5 wt. %, the peak for N-CH_3 which signified the existence of CTAB molecule shifted slightly to the right which was from 1407 cm^{-1} to 1409 cm^{-1}. The appearance of strong peaks at 1584 cm^{-1}, 1490 cm^{-1}, 1242 cm^{-1} and 1151 cm^{-1} interpreted the presence of C=C stretching, C-N stretching, C=O stretching and S=O stretching, respectively.

FIGURE 56: FTIR spectrum for membrane PSP1-C2.5

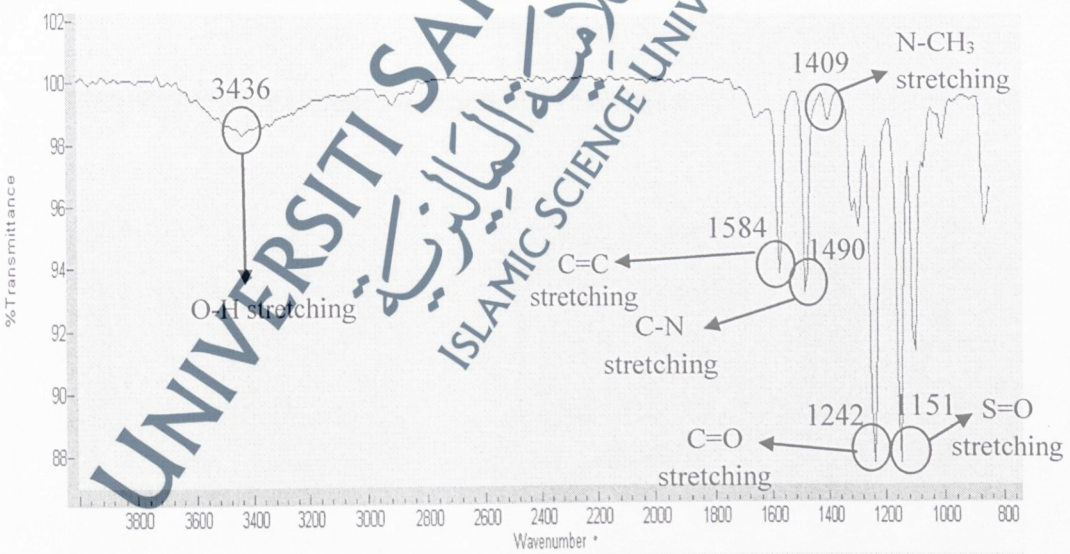

12) Membrane PSP1-C3.0

From FTIR spectrum for membrane PSP1-C3.0 (Figure 57), the transmittance band observed near 3477 cm^{-1} was attributed to the presence of O-H bond of PSF polymer, shifted to the left from those obtained in membrane PSP1 (3412 cm^{-1}). The appearance of peak at 1408 cm^{-1} in the spectrum confirmed the presence of N-CH_3 group, which was the important peak for CTAB. It is nearly the same as membrane PSP1-C1.0 which indicated that by increasing of CTAB concentration, the intensity of peak observed not significantly affected. The intense peaks observed at 1579 cm^{-1}, 1486 cm^{-1}, 1242 cm^{-1} and 1151 cm^{-1} were ascribed to the existence of C=C stretching, C-N stretching, C=O stretching and S=O stretching, respectively. Figure 58 showed the combination of FTIR spectra for membrane with different concentration of CTAB.

FIGURE 57: FTIR spectrum for membrane PSP1-C3.0

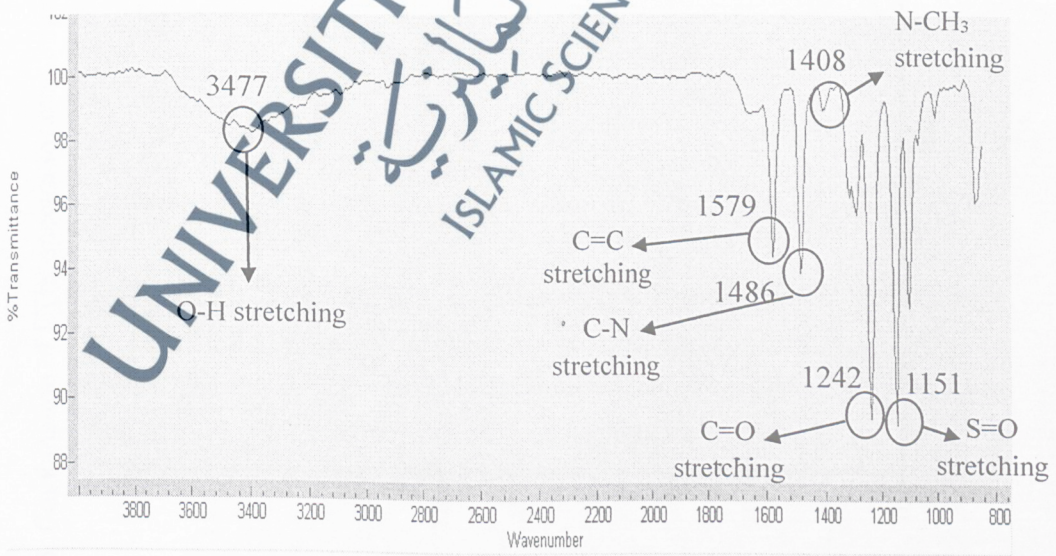

FIGURE 58: Combination of FTIR spectra for membranes with different concentration of CTAB

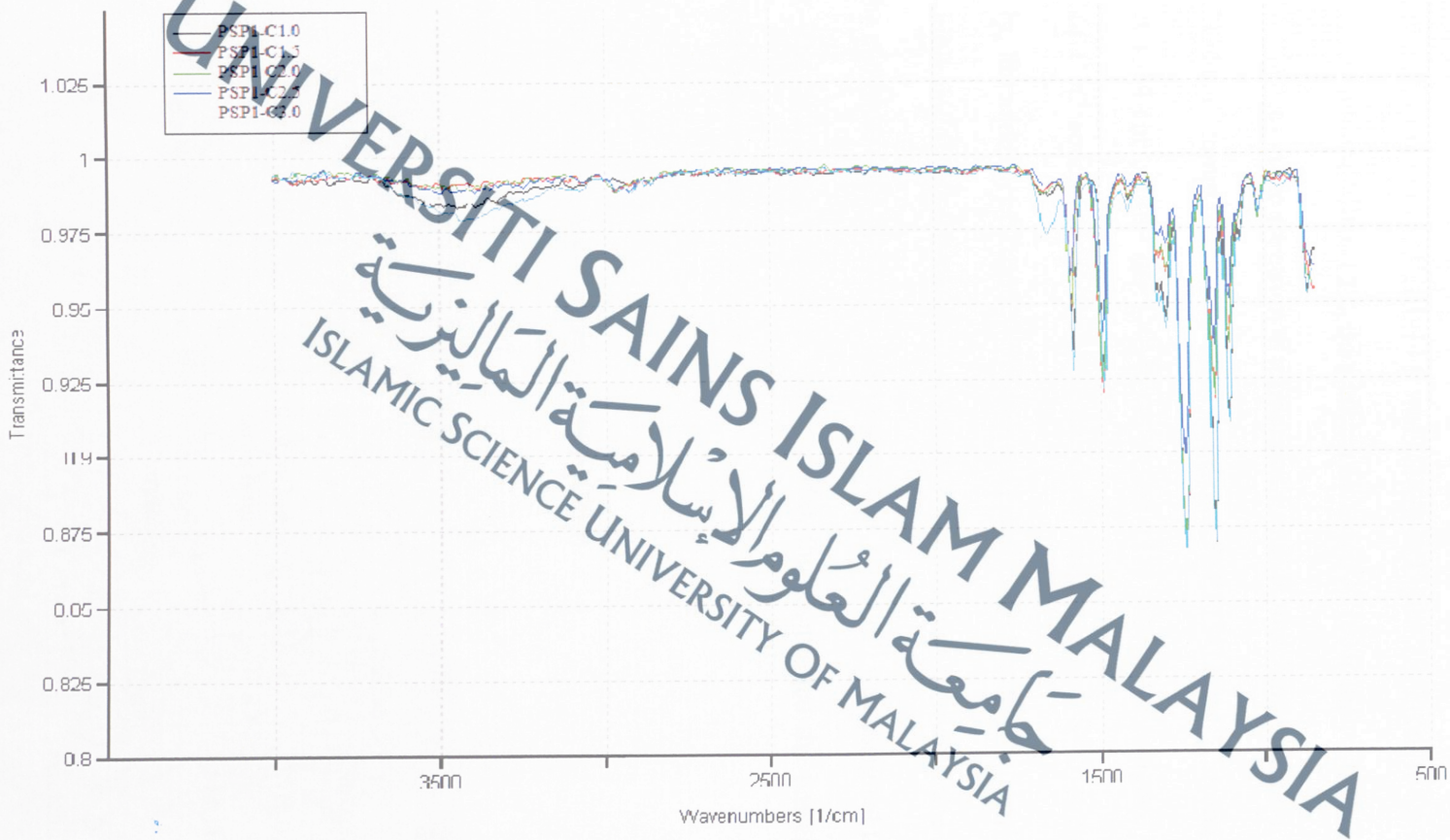

13) Membrane PSP1-T1.0

FTIR spectrum for membrane PSP1-T1.0 was shown in Figure 59. From the previous discussion on membrane PSP1-T2.0, the addition of Triton X-100 in the casting solution gave a slight changes in the spectrum of membrane. For O-H stretching vibration, it was shifted to 3454 cm^{-1} compared to the peak of membrane PSP1 (3412 cm^{-1}). Strong peaks appeared at 1584 cm^{-1}, 1489 cm^{-1}, 1242 cm^{-1} and 1151 cm^{-1} were assigned to the existence of C=C stretching, C-N stretching, C=O stretching and S=O stretching, respectively. The addition of Triton X-100 does not greatly affect those functional group as they exhibit almost the wavenumber as found in the spectrum of membrane PSP1. Instead, the significant transmittance band observed at 1105 cm^{-1} was assigned to C-O stretching. The C-O group belongs to Triton X-100, thus confirmed the presence of Triton X-100 in the membrane formulation.

FIGURE 59: FTIR spectrum for membrane PSP1-T1.0

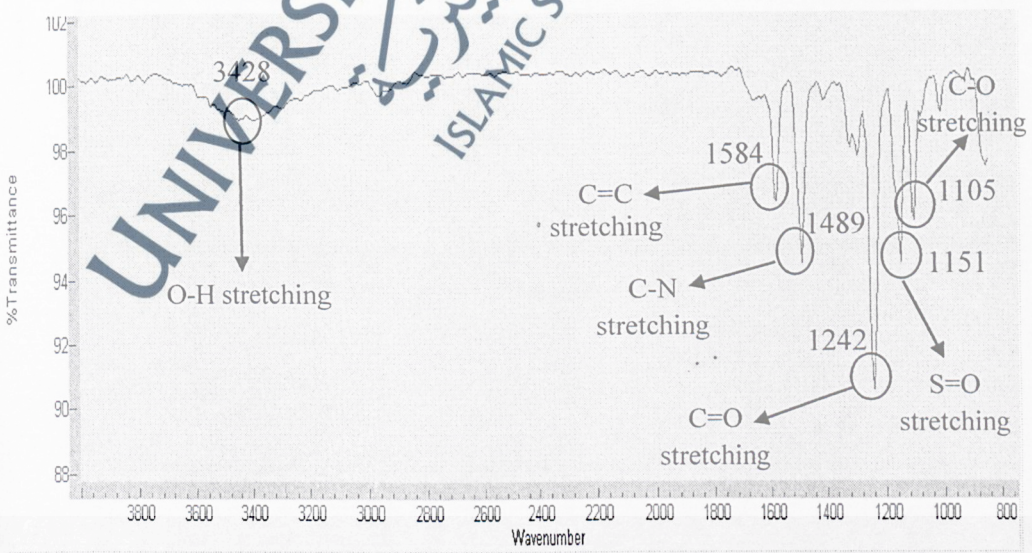

14) Membrane PSP1-T1.5

Figure 60 demonstrated the FTIR spectrum for membrane PSP1-T1.5. Increasing of Triton X-100 does not change the characteristic peak for Triton X-100 as it exhibit the C-O stretching at the peak of 1105 cm^{-1} which was similar in the spectrum of membrane PSP1-T1.0. Transmittance band observed at 3447 cm^{-1} ascribed as O-H stretching vibration of PSF polymer, shifted to the left by comparing with PSP1 (3412 cm^{-1}). The intense peaks observed at 1585 cm^{-1}, 1490 cm^{-1}, 1243 cm^{-1} and 1151 cm^{-1} were recognized to the existence of C=C stretching, C-N stretching, C=O stretching and S=O stretching, respectively.

FIGURE 60: FTIR spectrum for membrane PSP1-T1.5

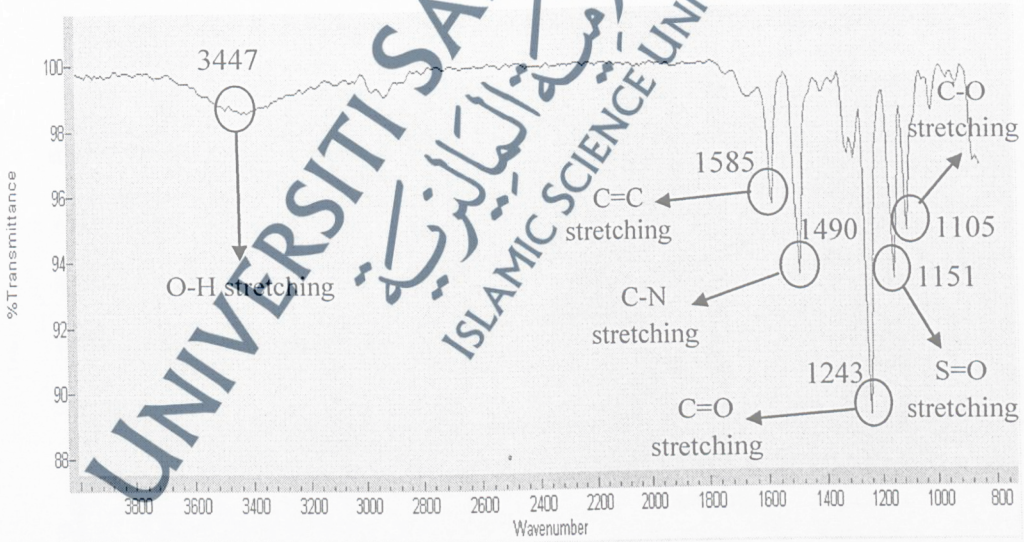

15) Membrane PSP1-T2.5

FTIR spectrum for membrane PSP1-T2.5 was shown in Figure 61. The transmittance band observed near 3432 cm^{-1} was assigned to O-H stretching vibration of PSF polymer. The strong peaks found at 1584 cm^{-1}, 1489 cm^{-1}, 1242 cm^{-1} and 1151 cm^{-1} were due to the stretching of C=C, C-N, C=O and S=O groups, respectively. The addition of Triton X-100 does not greatly affect those functional group as they exhibit almost the wavenumber as found in the spectrum of membrane PSP1. Moreover, C-O stretching for Triton X-100 molecules interpreted at the peak of 1105 cm^{-1} which was similar to the spectrum of PSP1-T1.0. It was indicated that increasing the concentration of Triton X-100 not significantly affect the spectrum of the membrane.

FIGURE 61: FTIR spectrum for membrane PSP1-T2.5

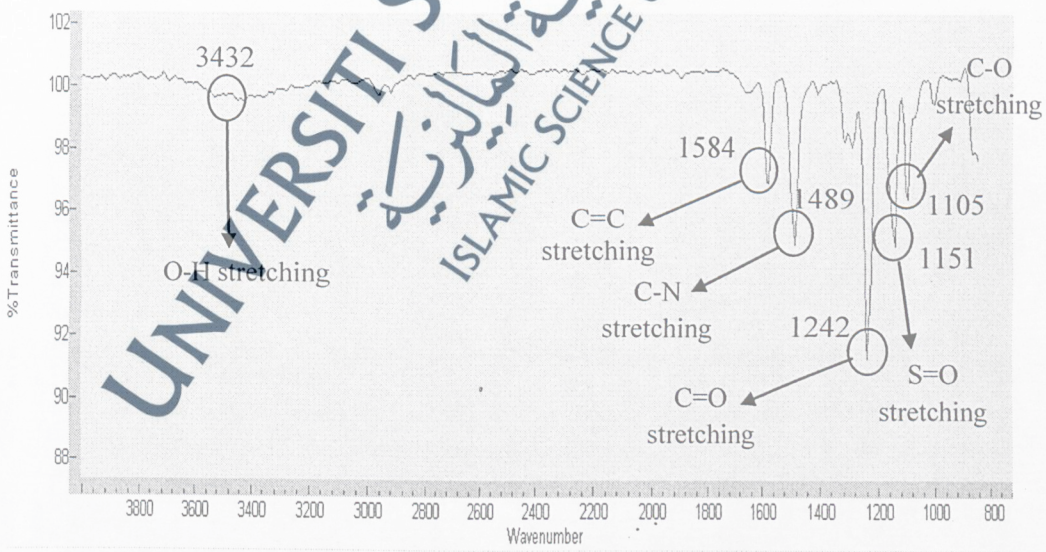

16) Membrane PSP1-T3.0

Figure 62 depicted the FTIR spectrum for membrane PSP1-T3.0. The O-H group of PSF showed a broad peak at 3448 cm^{-1} which was shifted to the left from membrane PSP1 (3412 cm^{-1}). For stretching of C=C, C-N, C=O and S=O groups, the strong peaks observed were similar to the peaks in spectrum for membrane PSP1 which were at 1585 cm^{-1}, 1490 cm^{-1}, 1243 cm^{-1} and 1151 cm^{-1}, respectively. Moreover, the existence of Triton X-100 in the membrane formulation confirmed by the interpretation of strong peak at 1106 cm^{-1} which belong to the C-O group of Triton X-100. It was slightly shifted from the peak in spectrum of membrane PSP1-T1.0. The combination of spectrum for membrane with different concentration of Triton X-100 was shown in Figure 63.

FIGURE 62: FTIR spectrum for membrane PSP1-T3.0

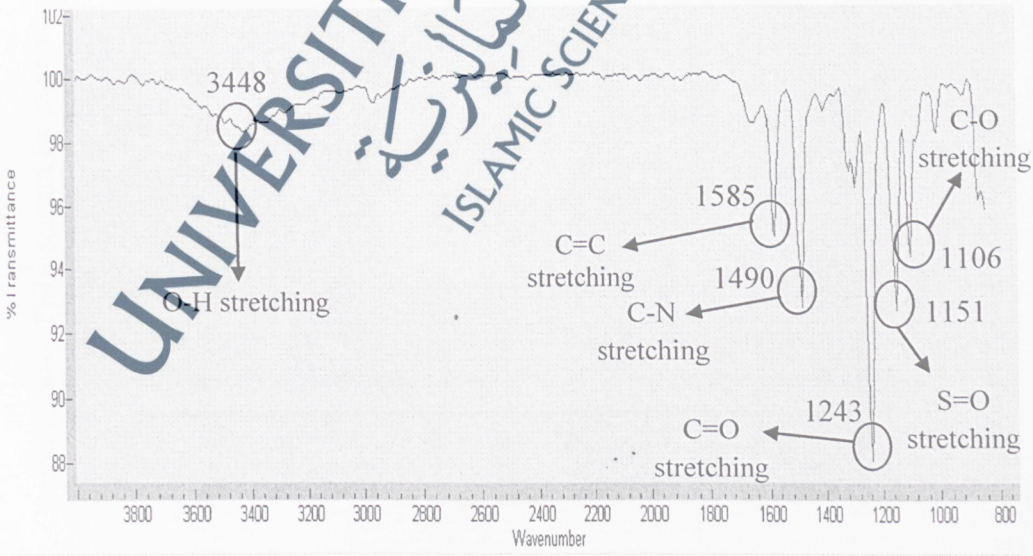

FIGURE 63: Combination of FTIR spectra for membranes with different concentration of Triton X-100

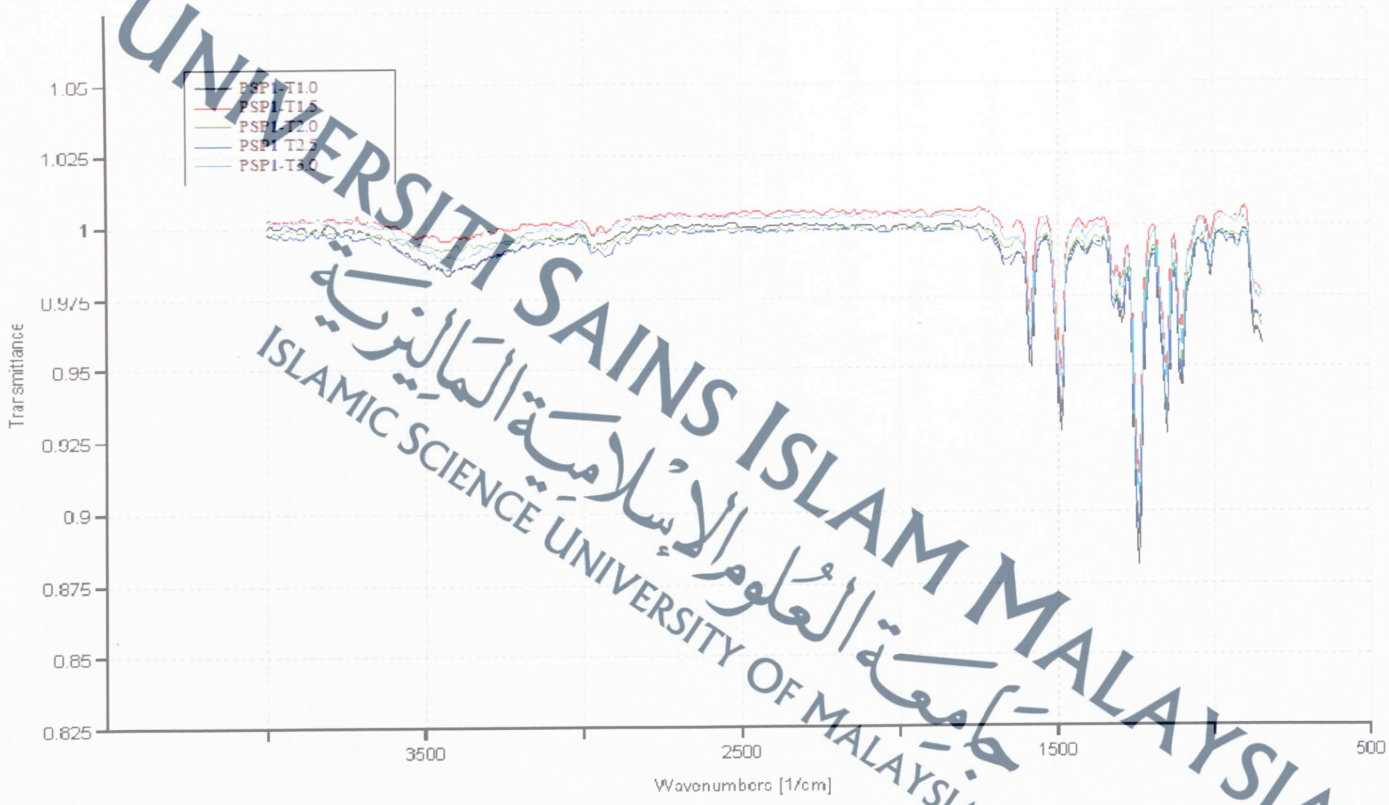

17) Membrane PSP1-S1.0

FTIR spectrum for membrane PSP1-S1.0 had been illustrated in Figure 64. For O-H stretching vibration, it was shifted to 3453 cm^{-1} by comparing with the spectrum of membrane PSP1 which was at 3412 cm^{-1} of wavenumber. The appearance of strong peaks at 1579 cm^{-1} and 1486 cm^{-1} were interpreted the presence of C=C stretching and C-N stretching, respectively. They were shifted to the right from both peaks in spectrum of membrane PSP1 which are 1585 cm^{-1} and 1490 cm^{-1}. For C=O stretching and S=O stretching, the intense peaks observed almost similar to those obtained in membrane PSP1 which are at 1242 cm^{-1} and 1151 cm^{-1}, respectively. Instead, an important peak was found at 2892 cm^{-1} which assigned to the $C-H_3$ stretching, revealed the existence of SDS molecule in the membrane solution.

FIGURE 64: FTIR spectrum for membrane PSP1-S1.0

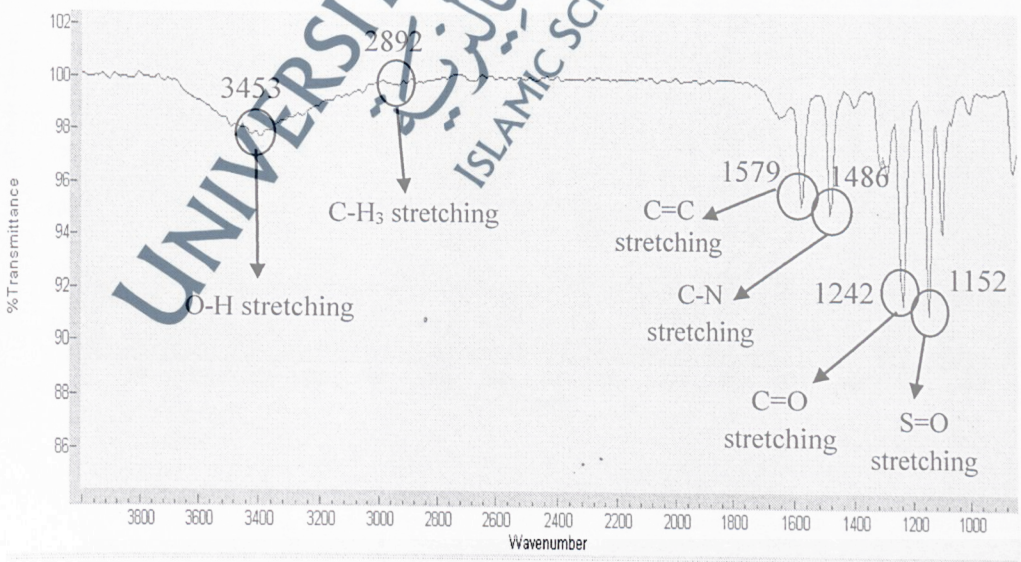

18) Membrane PSP1-S1.5

Figure 65 demonstrated the FTIR spectrum for membrane PSP1-S1.5. The transmittance band observed near 3476 cm^{-1} was assigned to O-H stretching vibration of PSF polymer, noticeable shifted to the left from the peak observed in spectrum of PSP1 (3412 cm^{-1}). The appearance of peak at 2866 cm^{-1} in the spectrum revealed the presence of $C-H_3$ group, which was the important peak for SDS. It is shifted to the right from the peak in spectrum of membrane PSP1-S1.0 which is at 2892 cm^{-1}. The strong peaks found at 1579 cm^{-1}, 1486 cm^{-1}, 1242 cm^{-1} and 1152 cm^{-1} were due to the stretching of C=C, C-N, C=O and S=O groups, respectively.

FIGURE 65: FTIR spectrum for membrane PSP1-S1.5

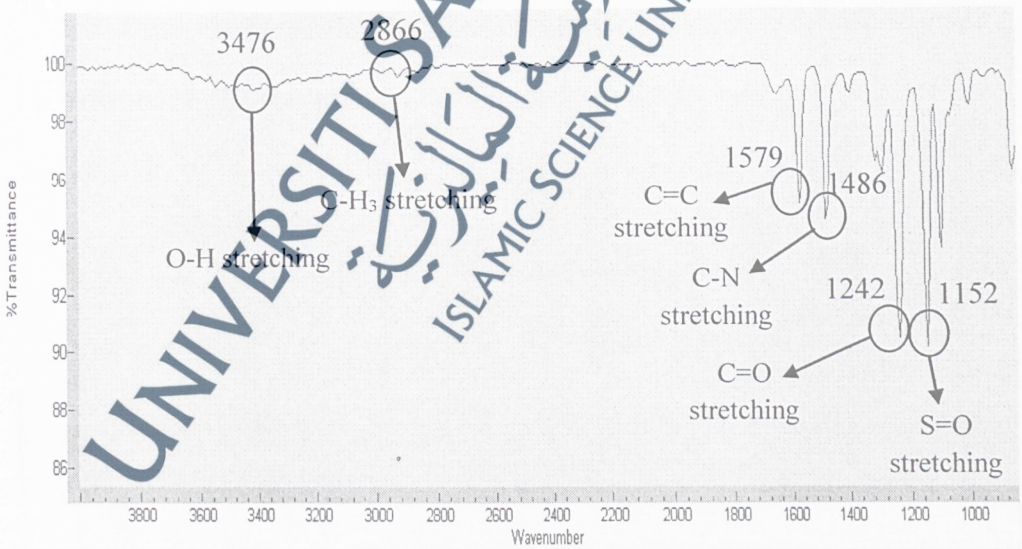

19) Membrane PSP1-S2.5

Figure 66 showed the FTIR spectrum for membrane PSP1-S2.5. Similar to the membrane PSP1-S1.5 that had been described previously, addition of small amount of SDS slightly changed the spectrum of the membrane. In this spectrum, the O-H stretching for PSF polymer was interpreted at the wavenumber of 3492 cm^{-1}, significantly shifted to the left from those found in pure PSF membrane (PSP1) which was 3412 cm^{-1}. By increasing the concentration of SDS, the characteristic peak for SDS which was for C-H_3 stretching interpreted shifted to the left from the peak in spectrum of membrane PSP1-S1.5 which was 2878 cm^{-1}. The C=C stretching, C-N stretching, C=O stretching and S=O stretching of PSF polymer were interpreted at 1579 cm^{-1}, 1484 cm^{-1}, 1242 cm^{-1}, and 1151 cm^{-1}, respectively which were nearly the same as those peaks obtained in membrane PSP1.

FIGURE 66: FTIR spectrum for membrane PSP1-S2.5

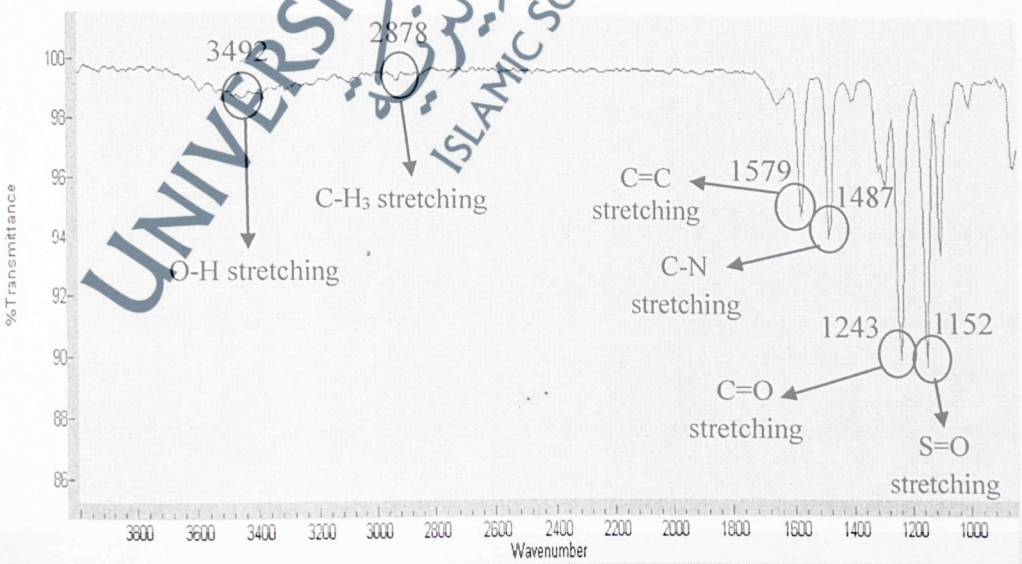

20) Membrane PSP1-S3.0

From FTIR spectrum for membrane PSP1-S3.0 (Figure 67), the transmittance band observed near 3423 cm^{-1} was attributed to the presence of O-H bond of PSF polymer, slightly from the peak in spectrum of membrane PSP1 (3412 cm^{-1}). The appearance of peak at 2867 cm^{-1} in the spectrum confirmed the presence of $C-H_3$ group, which was the important peak for SDS, shifted to the right from those obtained in membrane PSP1-S2.5. It was indicated that by varying the concentration of SDS, the characteristic peak for the spectrum was significantly affected. The intense peaks observed at 1579 cm^{-1}, 1487 cm^{-1}, 1243 cm^{-1} and 1152 cm^{-1} were ascribed to the existence of C=C stretching, C-N stretching, C=O stretching and S=O stretching, respectively. Figure 68 showed the combination of FTIR spectra for membrane with different concentration of SDS.

FIGURE 67: FTIR spectrum for membrane PSP1-S3.0

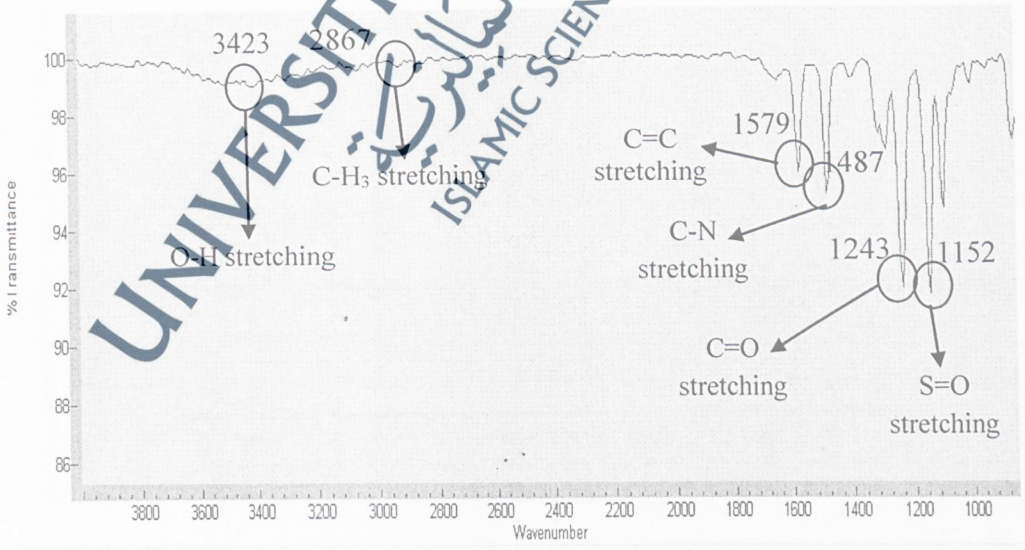

FIGURE 68: Combination of FTIR spectra for LPRO membrane with different concentration of SDS